Axisymmetric flows on the torus geometry – Supplementary Material (SM)–

Sergiu Busuioc[1], and H. Kusumaatmaja[2],† and Victor E. Ambruș[3,4]‡

[1]School of Engineering, University of Edinburgh, Edinburgh, EH9 3FB, UK

[2]Department of Physics, Durham University, Durham, DH1 3LE, UK

[3]Department of Physics, West University of Timișoara, Timișoara, 300223, Romania

[4]Department of Mathematics and Statistics,
Old Dominion University, Norfolk, VA 23529, USA

SM:1. Numerical implementation

In this section, the numerical method employed in this paper is described. In Subsec. SM:1.1, the governing equations are written collectively, in a manner suitable for the implementation of the flux vector splitting (FVS) method (Toro 2009). The time-stepping algorithm, described in Subsec. SM:1.2, is based on the explicit third order total variation diminishing (TVD) Runge-Kutta (RK-3) algorithm introduced by Shu & Osher (1988). The details concerning the implementation of the advection, which is performed using the fifth-order weighted essentially non-oscillatory (WENO-5) scheme (Jiang & Shu 1996), are given in Subsec. SM:1.3. The details concerning the implementation of the FVS (the Jacobian matrix, its eigenvectors and its eigenvalues) are also presented therein. Finally, Subsec. SM:1.4 discusses the implementation of the source terms. The numerical scheme presented herein is benchmarked against the flows discussed in Sections 3, 4 and 5 of the main text in Appendix A (also in the main text).

SM:1.1. *Governing equations*

The numerical implementation of the hydrodynamic equations (Eqs. (2.36), (2.41) and (2.43)), as well as of the Cahn-Hilliard equation (Eq. (2.44)), is based on the Flux Vector Splitting method (Toro 2009). These equations can be collectively written as:

$$\frac{\partial \mathbf{U}}{\partial t} + \frac{\partial_\theta[\mathbf{F}_\theta(\mathbf{U})]}{r(1+a\cos\theta)} + \frac{\partial_\varphi[\mathbf{F}_\varphi(\mathbf{U})]}{R(1+a\cos\theta)} = \mathbf{S}_{\rm inv} + \mathbf{S}_{\rm visc} + \mathbf{S}_{\rm CH}, \tag{SM:1.1}$$

where the derivative with respect to φ was included for completeness (axisymmetry is achieved by replacing all derivatives with respect to φ by 0). The conserved variables $\mathbf{U}$ and the flux vectors $\mathbf{F}_\theta(\mathbf{U})$ and $\mathbf{F}_\varphi(\mathbf{U})$ appearing on the left hand side of the above

† Email address for correspondence: halim.kusumaatmaja@durham.ac.uk
‡ Email address for correspondence: victor.ambrus@e-uvt.ro

relation satisfy:

$$\mathbf{U} = \begin{pmatrix} \rho \\ \rho u^{\hat{\theta}} \\ \rho u^{\hat{\varphi}} \\ \rho e + \frac{1}{2}\rho \boldsymbol{u}^2 \\ \phi \end{pmatrix}, \qquad \frac{\mathbf{F}_\theta(\mathbf{U})}{1 + a\cos\theta} = \begin{pmatrix} \rho u^{\hat{\theta}} \\ \rho (u^{\hat{\theta}})^2 + P_\mathrm{b} \\ \rho u^{\hat{\varphi}} u^{\hat{\theta}} \\ \rho h_t u^{\hat{\theta}} \\ \phi u^{\hat{\theta}} \end{pmatrix}, \qquad \mathbf{F}_\varphi(\mathbf{U}) = \begin{pmatrix} \rho u^{\hat{\varphi}} \\ \rho u^{\hat{\varphi}} u^{\hat{\theta}} \\ \rho (u^{\hat{\varphi}})^2 + P_\mathrm{b} \\ \rho h_t u^{\hat{\varphi}} \\ \phi u^{\hat{\varphi}} \end{pmatrix}, \tag{SM:1.2}$$

where ρ, $u^{\hat{\imath}} \in \{u^{\hat{\theta}}, u^{\hat{\varphi}}\}$, P_b, e and ϕ are the mass density, components of the fluid velocity, bulk pressure, specific energy and the order parameter, respectively. The total specific enthalpy h_t is written in terms of the specific enthalpy h and the fluid velocity as follows:

$$h_t = h + \frac{\boldsymbol{u}^2}{2}, \qquad h = e + \frac{P_\mathrm{b}}{\rho}. \tag{SM:1.3}$$

The source function is split into three contributions, corresponding to the inviscid terms due to the connection coefficients on the torus manifold, the viscous terms for non-perfect fluids and the terms for multicomponent flows, as follows:

$$\mathbf{S}_\mathrm{inv} = \frac{a\rho\sin\theta}{r(1+a\cos\theta)} \begin{pmatrix} 0 \\ -[(u^{\hat{\varphi}})^2 + P_\mathrm{b}/\rho] \\ u^{\hat{\varphi}} u^{\hat{\theta}} \\ 0 \\ 0 \end{pmatrix}, \qquad \mathbf{S}_\mathrm{visc} = \begin{pmatrix} 0 \\ \nabla_{\hat{\jmath}} \tau^{\hat{\theta}\hat{\jmath}} \\ \nabla_{\hat{\jmath}} \tau^{\hat{\varphi}\hat{\jmath}} \\ \mathrm{k}\Delta T + \nabla_{\hat{\imath}}(\tau^{\hat{\imath}\hat{\jmath}} u_{\hat{\jmath}}) \\ 0 \end{pmatrix},$$

$$\mathbf{S}_\mathrm{CH} = \begin{pmatrix} 0 \\ -\nabla_{\hat{\jmath}} \mathsf{P}_\kappa^{\hat{\theta}\hat{\jmath}} \\ -\nabla_{\hat{\jmath}} \mathsf{P}_\kappa^{\hat{\varphi}\hat{\jmath}} \\ -\nabla_{\hat{\imath}} (\mathsf{P}_\kappa^{\hat{\imath}\hat{\jmath}} u_{\hat{\jmath}}) \\ M\Delta\mu \end{pmatrix}. \tag{SM:1.4}$$

In the non-axially symmetric case, the dynamic part of the viscous stress receives an extra contribution compared to Eq. (2.37), as follows:

$$\begin{aligned} \tau^{\hat{\theta}\hat{\theta}}_\mathrm{dyn} = -\tau^{\hat{\varphi}\hat{\varphi}}_\mathrm{dyn} &= \eta \left[\frac{1+a\cos\theta}{r} \frac{\partial}{\partial\theta} \left(\frac{u^{\hat{\theta}}}{1+a\cos\theta} \right) - \frac{\partial_\varphi u^{\hat{\varphi}}}{R(1+a\cos\theta)} \right], \\ \tau^{\hat{\theta}\hat{\varphi}}_\mathrm{dyn} = \tau^{\hat{\varphi}\hat{\theta}}_\mathrm{dyn} &= \eta \left[\frac{1+a\cos\theta}{r} \frac{\partial}{\partial\theta} \left(\frac{u^{\hat{\varphi}}}{1+a\cos\theta} \right) + \frac{\partial_\varphi u^{\hat{\theta}}}{R(1+a\cos\theta)} \right], \end{aligned} \tag{SM:1.5}$$

while the bulk (volumetric) part is given by:

$$\tau^{\hat{\theta}\hat{\theta}}_\mathrm{bulk} = \tau^{\hat{\varphi}\hat{\varphi}}_\mathrm{bulk} = \eta_v \left[\frac{\partial_\theta [u^{\hat{\theta}}(1+a\cos\theta)]}{r(1+a\cos\theta)} + \frac{\partial_\varphi u^{\hat{\varphi}}}{R(1+a\cos\theta)} \right], \tag{SM:1.6}$$

with $\tau^{\hat{\theta}\hat{\varphi}}_\mathrm{bulk} = \tau^{\hat{\varphi}\hat{\theta}}_\mathrm{bulk} = 0$. The divergence of $\tau^{\hat{\imath}\hat{\jmath}}$ is computed via:

$$\begin{aligned} \nabla_{\hat{\jmath}} \tau^{\hat{\theta}\hat{\jmath}} &= \frac{\partial_\theta [\tau^{\hat{\theta}\hat{\theta}}_\mathrm{dyn} (1+a\cos\theta)^2]}{r(1+a\cos\theta)^2} + \frac{1}{r} \frac{\partial \tau^{\hat{\theta}\hat{\theta}}_\mathrm{bulk}}{\partial\theta} + \frac{\partial_\varphi \tau^{\hat{\theta}\hat{\varphi}}}{R(1+a\cos\theta)}, \\ \nabla_{\hat{\jmath}} \tau^{\hat{\varphi}\hat{\jmath}} &= \frac{\partial_\theta [\tau^{\hat{\theta}\hat{\varphi}} (1+a\cos\theta)^2]}{r(1+a\cos\theta)^2} + \frac{\partial_\varphi \tau^{\hat{\varphi}\hat{\varphi}}}{R(1+a\cos\theta)}. \end{aligned} \tag{SM:1.7}$$

The contributions to the Cahn-Hilliard source terms are

$$\nabla_{\hat{\jmath}}\mathsf{P}_\kappa^{\hat{\theta}\hat{\jmath}} = -\frac{\phi\kappa}{r}\frac{\partial(\Delta\phi)}{\partial\theta}, \qquad \nabla_{\hat{\jmath}}\mathsf{P}_\kappa^{\hat{\varphi}\hat{\jmath}} = -\frac{\phi\kappa\partial_\varphi(\Delta\phi)}{R(1+a\cos\theta)}. \tag{SM:1.8}$$

For the energy equation, the contribution to S_{visc} is computed using

$$\nabla_{\hat{\imath}}(\tau^{\hat{\imath}\hat{\jmath}}u_{\hat{\jmath}}) = \frac{\partial_\theta[\tau^{\hat{\theta}\hat{\jmath}}u_{\hat{\jmath}}(1+a\cos\theta)]}{r(1+a\cos\theta)} + \frac{\partial_\varphi(\tau^{\hat{\varphi}\hat{\jmath}}u_{\hat{\jmath}})}{R(1+a\cos\theta)}. \tag{SM:1.9}$$

A similar contribution appears in the energy equation due to the surface tension term, where $\tau^{\hat{\imath}\hat{\jmath}}$ is replaced by $-\mathsf{P}_\kappa^{\hat{\imath}\hat{\jmath}}$. However, we do not consider the details of the implementation of such a term, since we only consider the Cahn-Hilliard model at constant temperature, when the energy equation is not required.

SM:1.2. *Time stepping*

We consider the implementation of the time stepping using the third-order total variation diminishing (TVD) Runge-Kutta (RK-3) method introduced by (Shu & Osher 1988). We consider a discretisation of the time variable using equal time steps δt, such that the time coordinate t after n iterations is given by:

$$t_n = n\delta t. \tag{SM:1.10}$$

Writing the evolution equations Eq. (SM:1.1) as

$$\partial_t\mathsf{U} = L[\mathsf{U}], \tag{SM:1.11}$$

the conserved variables U_{n+1} at time t_{n+1} can be obtained from their values at time t_n using the following intermediate steps:

$$\begin{aligned}
\mathsf{U}_n^{(1)} =& \mathsf{U}_n + \delta t\, L[\mathsf{U}_n],\\
\mathsf{U}_n^{(2)} =& \frac{3}{4}\mathsf{U}_n + \frac{1}{4}\mathsf{U}_n^{(1)} + \frac{1}{4}\delta t\, L[\mathsf{U}_n^{(1)}],\\
\mathsf{U}_{n+1} =& \frac{1}{3}\mathsf{U}_n + \frac{2}{3}\mathsf{U}_n^{(2)} + \frac{2}{3}\delta t\, L[\mathsf{U}_n^{(2)}].
\end{aligned} \tag{SM:1.12}$$

SM:1.3. *Advection*

In Sec. 3, it was shown that in the linearised limit, the flow corresponding to constant ρ, P_{b} and e, vanishing $u^{\hat{\varphi}}$ and the incompressible velocity profile $u^{\hat{\theta}}(1+a\cos\theta) = \text{const}$ satisfies the linearised limit of the Euler equations. The strategy for the implementation of the advection step must be chosen such that this property is preserved also numerically.

The θ dimension is discretised using N_θ cells of equal size $\delta\theta = 2\pi/N_\theta$, centred on θ_s $(1 \leqslant s \leqslant N_\theta)$, where

$$\theta_s = \frac{2\pi}{N_\theta}\left(s - \frac{1}{2}\right). \tag{SM:1.13}$$

For $2D$ flows, the φ coordinate is similarly discretised using N_φ equally sized cells, centred on

$$\varphi_q = \frac{2\pi}{N_\varphi}\left(q - \frac{1}{2}\right), \tag{SM:1.14}$$

where $1 \leqslant q \leqslant N_\varphi$.

The advection is performed using a dimensionally-unsplit flux based approach, by

writing

$$\left\{\frac{\partial_\theta[\mathbf{F}_\theta(\mathbf{U})]}{r(1+a\cos\theta)}\right\}_{s,q} = \frac{\mathbf{F}^\theta_{s+1/2,q} - \mathbf{F}^\theta_{s-1/2,q}}{r(1+a\cos\theta_s)\delta\theta}, \tag{SM:1.15}$$

where $\mathbf{F}^\theta_{s\pm1/2,q}$ represent the fluxes reconstructed at the cell interfaces. Since the factor $1+a\cos\theta$, is included in the fluxes, the solution $u^{\hat{\theta}}(1+a\cos\theta) = \text{const}$ is an acceptable numerical solution of the linearised limit of the Euler equations. Similarly, the advection with respect to φ is performed using

$$\left\{\frac{\partial_\varphi[\mathbf{F}_\varphi(\mathbf{U})]}{R(1+a\cos\theta)}\right\}_{s,q} = \frac{\mathbf{F}^\varphi_{s,q+1/2} - \mathbf{F}^\varphi_{s,q-1/2}}{R(1+a\cos\theta_s)\delta\varphi}. \tag{SM:1.16}$$

The flux reconstruction is performed using the fifth order weighted essentially non-oscillatory (WENO-5) scheme proposed by Jiang & Shu (1996). The details of this reconstruction can be found in numerous papers, so we omit them here. In order to ensure the reconstruction of the fluxes in the upwind direction, we use the characteristic-wise flux-splitting finite-difference scheme (Shu 1997; Zhang & MacFadyen 2006; Radice & Rezzolla 2012). In order to use this approach, we focus on the advection with respect to θ and introduce the Jacobian matrix $\mathbf{A}_\theta \equiv \mathbf{A}_\theta(\mathbf{U})$ through:

$$\mathbf{A}_\theta = \frac{1}{1+a\cos\theta}\frac{\partial \mathbf{F}_\theta}{\partial \mathbf{U}}. \tag{SM:1.17}$$

At the interface $(s+1/2,q)$ and between the cells (s,q) and $(s+1,q)$, $\mathbf{A}^\theta_{s+1/2,q} \equiv \mathbf{A}_\theta(\mathbf{U}_{s+1/2,q})$ is computed using the arithmetic mean of the conserved variables to the left and right of the interface (Shu 1997; Radice & Rezzolla 2012; Rezzolla & Zanotti 2013):

$$\mathbf{U}_{s+1/2,q} = \frac{1}{2}(\mathbf{U}_{s,q} + \mathbf{U}_{s+1,q}). \tag{SM:1.18}$$

After finding the eigenvalues and eigenvectors of $\mathsf{A}^\theta_{s+1/2,q}$, the following decomposition is made:

$$\mathbf{A}^\theta_{s+1/2,q} = \mathbf{R}^\theta_{s+1/2,q}\boldsymbol{\Lambda}^\theta_{s+1/2,q}\mathbf{L}^\theta_{s+1/2,q}, \tag{SM:1.19}$$

where $\mathbf{R}^\theta_{s+1/2,q}$ and $\mathbf{L}^\theta_{s+1/2,q}$ are the matrices comprised of the right and left eigenvectors of $\mathbf{A}^\theta_{s+1/2,q}$, and $\boldsymbol{\Lambda}^\theta_{s+1/2,q}$ is a diagonal matrix containing the eigenvalues of $\mathbf{A}^\theta_{s+1/2,q}$, such that

$$\mathbf{AR} = \mathbf{R}\boldsymbol{\Lambda}, \qquad \mathbf{LA} = \boldsymbol{\Lambda}\mathbf{L}, \qquad \mathbf{LR} = \mathbf{I}. \tag{SM:1.20}$$

Then, the local characteristic fluxes $\mathbf{Q}^\theta_{s',q}$ are constructed as follows:

$$\mathbf{Q}^\theta_{s',q} = \mathbf{L}^\theta_{s+1/2,q}\mathbf{F}^\theta_{s',q}, \tag{SM:1.21}$$

where s' takes values between $s-3$ and $s+3$, covering the stencil employed for the WENO-5 reconstruction for the interface at $s+1/2$. The flux reconstruction is performed at the level of the characteristic fluxes and $\mathsf{Q}^{\theta;a}_{s+1/2,q}$ $(1 \leqslant a \leqslant 5)$ is obtained in an upwind-biased manner based on the sign of the a eigenvalue $(\Lambda^\theta_{s+1/2,q})_{a,a}$. The right eigenvectors are then used to obtain the fluxes corresponding to the conserved variables:

$$\mathbf{F}^\theta_{s+1/2,q} = \mathbf{R}^\theta_{s+1/2,q}\mathbf{Q}^\theta_{s+1/2,q}. \tag{SM:1.22}$$

We give below the details concerning the Jacobian $\mathbf{A}_\theta$, its eigenvalues and its left and right eigenvectors. Denoting by:

$$\mathbf{U} = (u_1, u_2, u_3, u_4, u_5)^T, \tag{SM:1.23}$$

where $u_1 = \rho$, $u_2 = \rho u^{\hat{\theta}}$, $u_3 = \rho u^{\hat{\varphi}}$, $u_4 = \rho e + \frac{1}{2}\rho \boldsymbol{u}^2$ and $u_5 = \phi$, the following relations can be found:

$$\frac{\partial P_{\mathrm{b}}}{\partial u_1} = P_\rho - \left(\frac{e}{\rho} - \frac{\boldsymbol{u}^2}{2\rho}\right) P_e, \qquad \frac{\partial P_{\mathrm{b}}}{\partial u_2} = -\frac{u^{\hat{\theta}} P_e}{\rho},$$
$$\frac{\partial P_{\mathrm{b}}}{\partial u_3} = -\frac{u^{\hat{\varphi}} P_e}{\rho}, \qquad \frac{\partial P_{\mathrm{b}}}{\partial u_4} = \frac{P_e}{\rho}, \qquad \frac{\partial P_{\mathrm{b}}}{\partial u_5} = P_\phi. \tag{SM:1.24}$$

The notations P_ρ, P_e and P_ϕ were introduced in Eq. (3.3). The Jacobian matrix is thus given by:

$$\mathbf{A}_\theta = \begin{pmatrix} 0 & 1 & 0 & 0 & 0 \\ -(u^{\hat{\theta}})^2 + P_\rho - (e - \frac{\boldsymbol{u}^2}{2})\frac{P_e}{\rho} & 2u^{\hat{\theta}} - \frac{u^{\hat{\theta}} P_e}{\rho} & -\frac{u^{\hat{\varphi}} P_e}{\rho} & \frac{P_e}{\rho} & P_\phi \\ -u^{\hat{\theta}} u^{\hat{\varphi}} & u^{\hat{\varphi}} & u^{\hat{\theta}} & 0 & 0 \\ -u^{\hat{\theta}}[h_t - P_\rho + (e - \frac{\boldsymbol{u}^2}{2})\frac{P_e}{\rho}] & h_t - \frac{(u^{\hat{\theta}})^2 P_e}{\rho} & -\frac{u^{\hat{\theta}} u^{\hat{\varphi}} P_e}{\rho} & \frac{u^{\hat{\theta}}(\rho + P_e)}{\rho} & u^{\hat{\theta}} P_\phi \\ -\frac{u^{\hat{\theta}}\phi}{\rho} & \frac{\phi}{\rho} & 0 & 0 & u^{\hat{\theta}} \end{pmatrix}. \tag{SM:1.25}$$

The eigenvalues of the Jacobian matrix $\mathbf{A}_\theta$ can be put in the following form:

$$\boldsymbol{\Lambda}_\theta = \mathrm{diag}(u^{\hat{\theta}} + c_s, u^{\hat{\theta}} - c_s, u^{\hat{\theta}}, u^{\hat{\theta}}, u^{\hat{\theta}}), \tag{SM:1.26}$$

where the speed of sound c_s is defined in Eq. (3.7). The right eigenvectors corresponding to $\Lambda^\theta_\pm = u^{\hat{\theta}} \pm c_s$ and $\Lambda^\theta_\varphi = \Lambda^\theta_e = \Lambda^\theta_\phi = u^{\hat{\theta}}$ are:

$$\mathbf{R}^\theta_\pm = \begin{pmatrix} 1 \\ u^{\hat{\theta}} \pm c_s \\ u^{\hat{\varphi}} \\ h_t \pm u^{\hat{\theta}} c_s \\ \phi/\rho \end{pmatrix}, \qquad \mathbf{R}^\theta_\varphi = \begin{pmatrix} 0 \\ 0 \\ 1 \\ u^{\hat{\varphi}} \\ 0 \end{pmatrix},$$
$$\mathbf{R}^\theta_e = \begin{pmatrix} 1 \\ u^{\hat{\theta}} \\ u^{\hat{\varphi}} \\ h_t + \frac{\phi P_\phi - \rho c_s^2}{P_e} \\ 0 \end{pmatrix}, \qquad \mathbf{R}^\theta_\phi = \begin{pmatrix} P_\phi \\ P_\phi u^{\hat{\theta}} \\ P_\phi u^{\hat{\varphi}} \\ P_\phi(h_t - e) \\ \frac{1}{\rho}(eP_e + \phi P_\phi) - c_s^2 \end{pmatrix}. \tag{SM:1.27}$$

The left eigenvectors satisfying $\mathbf{L}^{\theta;T}_\alpha \mathbf{R}^\theta_\beta = \delta_{\alpha\beta}$ for $\alpha, \beta \in \{+, -, \varphi, e, \phi\}$ are

$$\mathbf{L}^\theta_\pm = \frac{1}{2\rho c_s^2} \begin{pmatrix} \mp \rho c_s u^{\hat{\theta}} + \rho c_s^2 (1 - \Delta_P) \\ \pm \rho c_s - P_e u^{\hat{\theta}} \\ -P_e u^{\hat{\varphi}} \\ P_e \\ \rho P_\phi \end{pmatrix}, \qquad \mathbf{L}^\theta_\varphi = \begin{pmatrix} -u^{\hat{\varphi}} \\ 0 \\ 1 \\ 0 \\ 0 \end{pmatrix},$$
$$\mathbf{L}^\theta_e = \frac{P_e(\rho c_s^2 - eP_e)}{\rho c_s^2 P_\Delta} \begin{pmatrix} h - \frac{\boldsymbol{u}^2}{2} - \frac{e\phi P_\phi}{\rho c_s^2 - eP_e} \\ u^{\hat{\theta}} \\ u^{\hat{\varphi}} \\ -1 \\ \frac{\rho e P_\phi}{\rho c_s^2 - eP_e} \end{pmatrix}, \qquad \mathbf{L}^\theta_\phi = \frac{1}{\rho c_s^2 P_\Delta} \begin{pmatrix} \phi(\rho P_\rho - eP_e + P_e \frac{\boldsymbol{u}^2}{2}) \\ -\phi P_e u^{\hat{\theta}} \\ -\phi P_e u^{\hat{\varphi}} \\ \phi P_e \\ -\rho(\rho c_s^2 - \phi P_\phi) \end{pmatrix}, \tag{SM:1.28}$$

where the following notations were introduced:

$$\Delta_P = \frac{(2h - h_t)P_e + \phi P_\phi}{\rho c_s^2} = 1 - \frac{\rho P_\rho - eP_e + P_e \boldsymbol{u}^2/2}{\rho c_s^2}, \qquad P_\Delta = \rho c_s^2 - eP_e - \phi P_\phi. \tag{SM:1.29}$$

The Jacobian $\mathbf{A}_\varphi = \partial \mathbf{F}_\varphi / \partial \mathbf{U}$ can be obtained by performing the simultaneous permutation between the second and third lines, the second and third columns, as well as the flip $u^{\hat{\theta}} \leftrightarrow u^{\hat{\varphi}}$ in $\mathbf{A}_\theta$. It is given by:

$$\mathbf{A}_\varphi = \begin{pmatrix} 0 & 0 & 1 & 0 & 0 \\ -u^{\hat{\theta}} u^{\hat{\varphi}} & u^{\hat{\varphi}} & u^{\hat{\theta}} & 0 & 0 \\ -(u^{\hat{\varphi}})^2 + P_\rho - (e - \frac{\boldsymbol{u}^2}{2})\frac{P_e}{\rho} & -\frac{u^{\hat{\theta}} P_e}{\rho} & 2u^{\hat{\varphi}} - \frac{u^{\hat{\varphi}} P_e}{\rho} & \frac{P_e}{\rho} & P_\phi \\ -u^{\hat{\varphi}}[h_t - P_\rho + (e - \frac{\boldsymbol{u}^2}{2})\frac{P_e}{\rho}] & -\frac{u^{\hat{\theta}} u^{\hat{\varphi}} P_e}{\rho} & h_t - \frac{(u^{\hat{\varphi}})^2 P_e}{\rho} & \frac{u^{\hat{\varphi}}(\rho + P_e)}{\rho} & u^{\hat{\varphi}} P_\phi \\ -\frac{u^{\hat{\varphi}}\phi}{\rho} & 0 & \frac{\phi}{\rho} & 0 & u^{\hat{\varphi}} \end{pmatrix}. \tag{SM:1.30}$$

The eigenvalues of the Jacobian matrix $\mathbf{A}_\varphi$ can be put in the following form:

$$\boldsymbol{\Lambda}_\varphi = \mathrm{diag}(u^{\hat{\varphi}} + c_s, u^{\hat{\varphi}} - c_s, u^{\hat{\varphi}}, u^{\hat{\varphi}}, u^{\hat{\varphi}}), \tag{SM:1.31}$$

where the speed of sound c_s is defined in Eq. (3.7). The right eigenvectors corresponding to $\Lambda_\pm^\varphi = u^{\hat{\varphi}} \pm c_s$ and $\Lambda_\theta^\varphi = \Lambda_e^\varphi = \Lambda_\phi^\varphi = u^{\hat{\varphi}}$ are:

$$\mathbf{R}_\pm^\varphi = \begin{pmatrix} 1 \\ u^{\hat{\theta}} \\ u^{\hat{\varphi}} \pm c_s \\ h_t \pm u^{\hat{\varphi}} c_s \\ \phi/\rho \end{pmatrix}, \qquad \mathbf{R}_\theta^\varphi = \begin{pmatrix} 0 \\ 1 \\ 0 \\ u^{\hat{\theta}} \\ 0 \end{pmatrix},$$

$$\mathbf{R}_e^\varphi = \begin{pmatrix} 1 \\ u^{\hat{\theta}} \\ u^{\hat{\varphi}} \\ h_t + \frac{\phi P_\phi - \rho c_s^2}{P_e} \\ 0 \end{pmatrix}, \qquad \mathbf{R}_\phi^\varphi = \begin{pmatrix} P_\phi \\ P_\phi u^{\hat{\theta}} \\ P_\phi u^{\hat{\varphi}} \\ P_\phi(h_t - e) \\ \frac{1}{\rho}(eP_e + \phi P_\phi) - c_s^2 \end{pmatrix}. \tag{SM:1.32}$$

The left eigenvectors satisfying $\mathbf{L}_\alpha^{\varphi;T} \mathbf{R}_\beta^\varphi = \delta_{\alpha\beta}$ for $\alpha, \beta \in \{+, -, \theta, e, \phi\}$ are

$$\mathbf{L}_\pm^\varphi = \frac{1}{2\rho c_s^2} \begin{pmatrix} \mp \rho c_s u^{\hat{\varphi}} + \rho c_s^2 (1 - \Delta_P) \\ -P_e u^{\hat{\theta}} \\ \pm \rho c_s - P_e u^{\hat{\varphi}} \\ P_e \\ \rho P_\phi \end{pmatrix}, \qquad \mathbf{L}_\theta^\varphi = \begin{pmatrix} -u^{\hat{\theta}} \\ 1 \\ 0 \\ 0 \\ 0 \end{pmatrix},$$

$$\mathbf{L}_e^\varphi = \frac{P_e(\rho c_s^2 - eP_e)}{\rho c_s^2 P_\Delta} \begin{pmatrix} h - \frac{\boldsymbol{u}^2}{2} - \frac{e\phi P_\phi}{\rho c_s^2 - eP_e} \\ u^{\hat{\theta}} \\ u^{\hat{\varphi}} \\ -1 \\ \frac{\rho e P_\phi}{\rho c_s^2 - eP_e} \end{pmatrix}, \qquad \mathbf{L}_\phi^{\hat{\varphi}} = \frac{1}{\rho c_s^2 P_\Delta} \begin{pmatrix} \phi(\rho P_\rho - eP_e + P_e \frac{\boldsymbol{u}^2}{2}) \\ -\phi P_e u^{\hat{\theta}} \\ -\phi P_e u^{\hat{\varphi}} \\ \phi P_e \\ -\rho(\rho c_s^2 - \phi P_\phi) \end{pmatrix}, \tag{SM:1.33}$$

where the notations Δ_P and P_Δ were introduced in Eq. (SM:1.29).

SM:1.4. *Implementation of source terms*

The inviscid source term, $\mathbf{S}_{\rm inv}$, is computed by simply evaluating all quantities at $(\theta,\varphi)=(\theta_s,\varphi_q)$.

The viscous term is computed by noting that the profile $u^{\hat\varphi}\sim(1+a\cos\theta)$ is non-dissipative in the linearised limit of the Navier-Stokes equations, as discussed in Sec. 4. Thus, the components $\tau^{\hat\theta\hat\theta}_{\rm dyn}=-\tau^{\hat\varphi\hat\varphi}_{\rm dyn}$ and $\tau^{\hat\theta\hat\varphi}_{\rm dyn}$ are computed as:

$$\begin{aligned}\tau^{\hat\theta\hat\theta}_{{\rm dyn};s,q}=&\eta_{s,q}\left[\frac{1+a\cos\theta_s}{r}\left(\frac{\partial}{\partial\theta}\frac{u^{\hat\theta}}{1+a\cos\theta}\right)_{s,q}-\frac{(\partial_\varphi u^{\hat\varphi})_{s,q}}{R(1+a\cos\theta_s)}\right],\\ \tau^{\hat\theta\hat\varphi}_{{\rm dyn};s,q}=&\eta_{s,q}\left[\frac{1+a\cos\theta_s}{r}\left(\frac{\partial}{\partial\theta}\frac{u^{\hat\varphi}}{1+a\cos\theta}\right)_{s,q}+\frac{(\partial_\varphi u^{\theta})_{s,q}}{R(1+a\cos\theta_s)}\right],\end{aligned}\tag{SM:1.34}$$

where a centred fourth-order stencil is used to compute the θ and φ derivatives:

$$\begin{aligned}\left(\frac{\partial f}{\partial\theta}\right)_{s,q}=&\frac{1}{12\delta\theta}\left(-f_{s+2,q}+8f_{s+1,q}-8f_{s-1,q}+f_{s-2,q}\right),\\ \left(\frac{\partial f}{\partial\varphi}\right)_{s,q}=&\frac{1}{12\delta\varphi}(-f_{s,q+2}+8f_{s,q+1}-8f_{s,q-1}+f_{s,q-2}).\end{aligned}\tag{SM:1.35}$$

The bulk viscosity term is computed as follows:

$$\tau^{\hat\imath\hat\jmath}_{{\rm bulk};s,q}=\delta^{\hat\imath\hat\jmath}\eta_{v;s}\left[\frac{\partial_\theta[u^{\hat\theta}(1+a\cos\theta)]_{s,q}}{r(1+a\cos\theta_s)}+\frac{(\partial_\varphi u^{\hat\varphi})_{s,q}}{R(1+a\cos\theta_s)}\right],\tag{SM:1.36}$$

where the derivatives are computed using Eq. (SM:1.35). The divergence of the viscous stress $\tau^{\hat\imath\hat\jmath}$ is computed as follows:

$$\begin{aligned}(\nabla_{\hat\jmath}\tau^{\hat\theta\hat\jmath})_{s,q}=&\frac{\partial_\theta[\tau^{\hat\theta\hat\theta}_{\rm dyn}(1+a\cos\theta)^2]_{s,q}}{r(1+a\cos\theta_s)^2}+\frac{1}{r}\left(\frac{\partial\tau^{\hat\theta\hat\theta}_{\rm bulk}}{\partial\theta}\right)_{s,q}+\frac{(\partial_\varphi\tau^{\hat\theta\hat\varphi})_{s,q}}{R(1+a\cos\theta_s)},\\ (\nabla_{\hat\jmath}\tau^{\hat\varphi\hat\jmath})_{s,q}=&\frac{\partial_\theta[\tau^{\hat\theta\hat\varphi}(1+a\cos\theta)^2]_{s,q}}{r(1+a\cos\theta_s)^2}+\frac{(\partial_\varphi\tau^{\hat\varphi\hat\varphi})_{s,q}}{R(1+a\cos\theta_s)}.\end{aligned}\tag{SM:1.37}$$

where the stencil in Eq. (SM:1.35) is again used to compute the derivatives with respect to θ and φ.

Finally, the Laplacians of the temperature, order parameter and chemical potential can be computed as follows:

$$(\Delta f)_{s,q}=\frac{1}{r^2(1+a\cos\theta_s)^2}\left(\frac{\partial^2 f}{\partial\chi^2}\right)_{s,q}+\frac{1}{R^2(1+a\cos\theta_s)^2}\left(\frac{\partial^2 f}{\partial\varphi^2}\right)_{s,q},\tag{SM:1.38}$$

where the coordinate χ is defined as:

$$\chi(\theta)=\int_0^\theta\frac{d\theta}{1+a\cos\theta}=\frac{2}{\sqrt{1-a^2}}\arctan\left[\sqrt{\frac{1-a}{1+a}}\tan\frac{\theta}{2}\right].\tag{SM:1.39}$$

In the above, the arctangent is computed such that χ is continuous at π, where $\chi(\theta=\pi)=2\pi/\sqrt{1-a^2}$. A five-point stencil with respect to the non-equidistant coordinate χ is employed, such that (Ambruș *et al.* 2019):

$$\left(\frac{\partial^2 f}{\partial\chi^2}\right)_{s,q}=a_{s;2}f_{s+2,q}+a_{s;1}f_{s+1,q}++a_{s;0}f_{s,q}+a_{s;-1}f_{s-1,q}+a_{s;-2}f_{s-2,q},\tag{SM:1.40}$$

where the coefficients $a_{s;k}$ are given below:

$$a_{s;\pm 2} = \frac{2[(\chi_s - \chi_{s\mp 1})(\chi_s - \chi_{s\mp 2}) + (\chi_s - \chi_{s\pm 1})(2\chi_s - \chi_{s\mp 1} - \chi_{s\mp 2})]}{(\chi_{s\pm 2} - \chi_{s\mp 2})(\chi_{s\pm 2} - \chi_{s+1})(\chi_{s\pm 2} - \chi_s)(\chi_{s\pm 2} - \chi_{s-1})},$$
$$a_{s;\pm 1} = \frac{2[(\chi_s - \chi_{s\mp 1})(\chi_s - \chi_{s\mp 2}) + (\chi_s - \chi_{s\pm 2})(2\chi_s - \chi_{s\mp 1} - \chi_{s\mp 2})]}{(\chi_{s\pm 1} - \chi_{s\mp 1})(\chi_{s\pm 1} - \chi_{s+2})(\chi_{s\pm 1} - \chi_s)(\chi_{s\pm 1} - \chi_{s-2})}, \quad \text{(SM:1.41)}$$

while $a_{s;0} = -a_{s;2} - a_{s;1} - a_{s;-1} - a_{s;-2}$. The derivative with respect to φ appearing in Eq. (SM:1.38) is computed using:

$$\left(\frac{\partial^2 f}{\partial \varphi^2}\right)_{s,q} = \frac{1}{\delta\varphi^2}\left(-\frac{1}{12}f_{s,q+2} + \frac{4}{3}f_{s,q+1} - \frac{5}{2}f_{s,q} + \frac{4}{3}f_{s,q-1} - \frac{1}{12}f_{s,q-2}\right). \quad \text{(SM:1.42)}$$

SM:2. Stripe configurations and diffusive dynamics in Cahn-Hilliard binary fluids: Mathematical complements

This section contains mathematical complements linking the general analysis presented in Sections 6 and 7 of the main text to the Cahn-Hilliard model. Section SM:2.1 begins with the analysis of the Laplace-Young pressure law, discussed for the case of general fluids exhibiting an interface in Sec. 6 of the main text, highlighting that in the context of the Cahn-Hilliard model, this pressure difference induces a global offset, ϕ_0 of the order parameter. Next, Sec. SM:2.2 shows that, under the ansatz of a hyperbolic tangent profile of the order parameter, the conservation of the area of a stripe of the minority component embedded in the majority component is ensured through the Cahn-Hilliard equation up to terms of second order with respect to the ratio ξ_0/r between the interface width and the radius of the torus along the poloidal direction. Finally, under the same assumption for the order parameter profile, Sec. SM:2.3 provides the mathematical connection between the total free energy, introduced in Eq. (2.6) of the main text, and the total interface length of the stripe configuration. Finally, Sec. SM:2.4 discusses the drift dynamics of fluid stripes embedded on the torus geometry in the absence of hydrodynamics.

SM:2.1. *Offset of the order parameter and Laplace pressure law*

In this subsection, we consider the Laplace-Young pressure difference across the stripe interfaces, discussed in Sec. 6 of the main text, in the context of the Cahn-Hilliard model. Far away from the interface, the pressure tensor is diagonal, being dominated by the bulk contribution P_b, introduced in Eq. (2.11). Considering that in equilibrium, there are in principle no density or temperature gradients, the difference $\Delta P = P_\mathrm{in} - P_\mathrm{out}$ between the pressure inside and outside the stripe, given in Eq. (6.27) of the main text for the general case of a fluid stripe exhibiting interfaces with line tension σ, it is clear that there must exist a deviation of the order parameter ϕ from the expected values, ± 1, inside and/or outside the fluid stripe. We conjecture that this difference is a global offset of the order parameter, which we denote by ϕ_0, which is allowed since the torus is a periodic manifold (in the infinite Cartesian space, the order parameter must go to ± 1 at infinite distances from the enclosed domain). In lack of an analytic expression for the interface between the two components in the Cahn-Hilliard model on the torus geometry, we take the simplistic assumption that the profile of the order parameter is well described by a hyperbolic tangent (which is an exact solution for a flat interface on the infinite Cartesian space), with the addition of the constant value ϕ_0:

$$\phi = \phi_0 + \tanh\zeta, \qquad \zeta = \frac{r}{\xi_0\sqrt{2}}\left(\widetilde{|\theta-\theta_c|} - \frac{\Delta\theta}{2}\right), \tag{SM:2.1}$$

where θ_c represents the angular coordinate of the stripe centre, $r\Delta\theta$ represents its width and $\xi_0 = \sqrt{\kappa/A}$ is the interface width in the case of the flat geometry, according to Eq. (2.8). The notation $\widetilde{\theta-\theta_c}$ indicates that the angular difference $\theta - \theta_c$ takes values between $-\pi$ and π.

According to Eq. (SM:2.1), in the interior of the stripe, $\phi \simeq \phi_0 - 1$, while outside the stripe, $\phi \simeq \phi_0 + 1$. Up to second order terms, the pressure difference between the inside of the stripe and the outside of the stripe can be computed from Eq. (2.11):

$$\Delta P = -4\mathrm{A}\phi_0, \tag{SM:2.2}$$

where a term of order $O(\phi_0^3)$ was neglected.

In order to determine the value of ϕ_0, we start by evaluating the chemical potential $\mu = -\mathrm{A}\phi(1-\phi^2) - \kappa\Delta\phi$ (Eq. (2.9) in the main text), far away from the interface. Noting

that the gradient terms become negligible, μ reduces to:

$$\mu(\phi = \phi_0 \pm 1) \simeq 2\mathrm{A}\phi_0 \left(1 \pm \frac{3}{2}\phi_0 + \frac{1}{2}\phi_0^2\right) = \mathrm{A}\phi_0(2 + \phi_0^2) \pm 3\mathrm{A}\phi_0^2, \tag{SM:2.3}$$

where the upper (+) and lower (−) signs in the equation above refer to the exterior and interior of the stripe, respectively. Since in equilibrium, the only acceptable stationary solution corresponds to $\mu = \text{const}$, the term $\pm 3\mathrm{A}\phi_0^2$ must cancel due to correction terms to the order parameter profile which are not included in Eq. (SM:2.1). Thus, Eq. (SM:2.3) can be regarded as a good approximation for μ only up to first order with respect to ϕ_0.

We now consider the average value $\langle\mu\rangle$ of the chemical potential. The departure of the average value from 0 is due to the offset ϕ_0 of the order parameter, as well as to variations of the chemical potential around the interfaces. We conjecture that the value of ϕ_0 is such that these variations are minimised, which can be achieved by imposing:

$$\langle\mu\rangle \simeq 2\mathrm{A}\phi_0. \tag{SM:2.4}$$

It remains to compute $\langle\mu\rangle$. Noting that the Laplacian term, $\kappa\Delta\phi$, does not contribute to volume integrals, $\langle\mu\rangle$ reduces to:

$$\begin{aligned}
\langle\mu\rangle &= \int_0^{2\pi} \frac{d\theta}{2\pi}(1 + a\cos\theta)[-\mathrm{A}\phi(1-\phi)^2] = \langle\mu\rangle_{\text{bulk}} + \langle\mu\rangle_{\text{interface}}\,, \\
\langle\mu\rangle_{\text{bulk}} &\simeq \mathrm{A}\int_0^{2\pi} \frac{d\theta}{2\pi}(1 + a\cos\theta)(2\phi_0 + \phi_0^3 + 3\phi_0^2\mathrm{sgn}\zeta), \\
\langle\mu\rangle_{\text{interface}} &\simeq -\mathrm{A}\int_0^{2\pi} \frac{d\theta}{2\pi}(1 + a\cos\theta)\left(\frac{3\phi_0 + \tanh\zeta}{\cosh^2\zeta} + 3\phi_0^2\frac{e^{-|\zeta|}\mathrm{sgn}\zeta}{\cosh\zeta}\right),
\end{aligned} \tag{SM:2.5}$$

where two contributions, corresponding to bulk and interface terms, were identified in the expression for μ. The $\simeq$ signs indicate that the hyperbolic tangent approximation given in Eq. (SM:2.1) was used for the order parameter. In deriving the split into bulk and interface contributions, the following relation was employed:

$$\tanh\zeta = \mathrm{sgn}\zeta\left(1 - \frac{e^{-|\zeta|}}{\cosh\zeta}\right). \tag{SM:2.6}$$

In order to compute $\langle\mu\rangle_{\text{bulk}}$, the following integrals are required:

$$\int_0^{2\pi} \frac{d\theta}{2\pi}(1 + a\cos\theta) = 1, \tag{SM:2.7}$$

$$\begin{aligned}
\int_0^{2\pi} \frac{d\theta}{2\pi}(1 + a\cos\theta)\mathrm{sgn}\zeta &= \int_{-\pi}^{\pi} \frac{d\vartheta}{2\pi}[1 + a\cos(\vartheta + \theta_c)]\mathrm{sgn}(|\vartheta| - \Delta\theta/2) \\
&= 2\int_{-\Delta\theta/2}^{(2\pi-\Delta\theta)/2} \frac{d\varsigma}{2\pi}\left[1 + a\cos\theta_c\cos\left(\frac{\Delta\theta}{2} + \varsigma\right)\right]\mathrm{sgn}(\varsigma) \\
&= 1 - \frac{1}{\pi}\left(\Delta\theta + 2a\cos\theta_c\sin\frac{\Delta\theta}{2}\right),
\end{aligned} \tag{SM:2.8}$$

where the equality on the second line follows after changing the integration domain to $\theta_c - \pi \leqslant \theta \leqslant \theta_c + \pi$ and changing variables to $\vartheta = \theta - \theta_c$. On the third line, the integral is broken into the negative and positive ϑ domains and the two contributions are added together, after which the integration variable is changed to $\varsigma = \vartheta - (\Delta\theta/2)$. The result on the last line above is just $1 - 2\Delta A/A_{\text{total}}$, where $A_{\text{total}} = 4\pi^2 rR$ is the area of the torus, while ΔA is the stripe area, given by $\Delta A = 2\pi rR[\Delta\theta + 2a\sin(\Delta\theta/2)\cos\theta_c]$ (Eq. (6.2) in

the main text). Summing up the terms corresponding to the first set, we obtain:

$$\langle\mu\rangle_{\rm bulk} = \mathrm{A}\phi_0(2+\phi_0^2) + 3\mathrm{A}\phi_0^2\left(1 - \frac{2\Delta A}{A_{\rm total}}\right). \tag{SM:2.9}$$

Comparing Eq. (SM:2.9) with Eq. (SM:2.3), it can be seen that, to first order in ϕ_0, the bulk contribution to $\langle\mu\rangle$ matches the expected expression. Thus, the value of ϕ_0 must be chosen such that the interface contribution $\langle\mu\rangle_{\rm interface}$ cancels:

$$\langle\mu\rangle_{\rm interface} = 0. \tag{SM:2.10}$$

In order to compute $\langle\mu\rangle_{\rm interface}$, three integrals must be evaluated. The first one, corresponding to the term proportional to $1/\cosh^2\zeta$, can be simplified as follows:

$$\int_0^{2\pi}\frac{d\theta}{2\pi}(1+a\cos\theta)\frac{1}{\cosh^2\zeta} = \frac{\xi_0\sqrt{2}}{\pi r}\int_{-r\Delta\theta/\xi_0\sqrt{8}}^{r(2\pi-\Delta\theta)/\xi_0\sqrt{8}}\frac{d\zeta}{\cosh^2\zeta} \times\left[1+a\cos\theta_c\cos\left(\frac{\Delta\theta}{2}+\frac{\xi_0\zeta\sqrt{2}}{r}\right)\right], \tag{SM:2.11}$$

where the equality is obtained after performing the changes of variable employed in Eq. (SM:2.8), followed by a switch to $\zeta = r\varsigma/\xi_0\sqrt{2}$. Assuming now that the interface width is much smaller than the stripe width, i.e., $2\xi_0\sqrt{2} \ll r\Delta\theta$, the integration domain can be extended to infinity. In this case, the integration domain becomes symmetric with respect to ζ and only the even terms make non-vanishing contributions. This allows $\cos\left(\frac{\Delta\theta}{2}+\frac{\xi_0\zeta\sqrt{2}}{r}\right)$ to be replaced by $\cos\frac{\Delta\theta}{2}\cos\frac{\xi_0\zeta\sqrt{2}}{r}$. The integration with respect to ζ can be performed by noting that:

$$\int_{-\infty}^{\infty}\frac{d\zeta}{\cosh^2\zeta} = 2, \qquad \int_{-\infty}^{\infty}\frac{d\zeta}{\cosh^2\zeta}\cos(\beta\zeta) = \frac{\pi\beta}{\sinh(\pi\beta/2)}. \tag{SM:2.12}$$

Thus, we obtain:

$$\int_0^{2\pi}\frac{d\theta}{2\pi}(1+a\cos\theta)\frac{1}{\cosh^2\zeta} = \frac{\xi_0\sqrt{8}}{\pi r}\left[1+a\cos\theta_c\cos\frac{\Delta\theta}{2}\frac{\pi\xi_0/r\sqrt{2}}{\sinh(\pi\xi_0/r\sqrt{2})}\right]. \tag{SM:2.13}$$

The second integral to compute for the evaluation of $\langle\mu\rangle_{\rm interface}$ in Eq. (SM:2.5) corresponds to the term proportional to $\tanh\zeta/\cosh^2\zeta$, which can be simplified as follows:

$$\int_0^{2\pi}\frac{d\theta}{2\pi}(1+a\cos\theta)\frac{\tanh\zeta}{\cosh^2\zeta} \simeq \frac{a\xi_0\sqrt{2}}{\pi r}\cos\theta_c\int_{-\infty}^{\infty}\frac{\tanh\zeta\,d\zeta}{\cosh^2\zeta}\cos\left(\frac{\Delta\theta}{2}+\frac{\xi_0\zeta\sqrt{2}}{r}\right). \tag{SM:2.14}$$

Noting that the odd contributions with respect to ζ vanish, the cosine can be replaced with $[-\sin(\Delta\theta/2)\sin(\xi_0\zeta\sqrt{2}/r)]$. Using the relation:

$$\int_{-\infty}^{\infty}\frac{\tanh\zeta d\zeta}{\cosh^2\zeta}\sin(\beta\zeta) = \frac{\pi\beta^2/2}{\sinh(\pi\beta/2)}, \tag{SM:2.15}$$

the following result can be obtained:

$$\int_0^{2\pi}\frac{d\theta}{2\pi}(1+a\cos\theta)\frac{\tanh\zeta}{\cosh^2\zeta} \simeq -\frac{2a\xi_0^2}{\pi r^2}\cos\theta_c\sin\frac{\Delta\theta}{2}\frac{\pi\xi_0/r\sqrt{2}}{\sinh(\pi\xi_0/r\sqrt{2})}. \tag{SM:2.16}$$

Finally, the last integral required to compute $\langle\mu\rangle_{\rm interface}$ (SM:2.5) corresponds to the

term proportional to $e^{-|\zeta|}\mathrm{sgn}\zeta/\cosh\zeta$. This can be simplified as follows:

$$\int_0^{2\pi}\frac{d\theta}{2\pi}(1+a\cos\theta)\frac{e^{-|\zeta|}\mathrm{sgn}\zeta}{\cosh\zeta}\simeq-\frac{2a\xi_0\sqrt{2}}{\pi r}\cos\theta_c\sin\frac{\Delta\theta}{2}\int_0^{\infty}\frac{e^{-\zeta}d\zeta}{\cosh\zeta}\sin\frac{\xi_0\zeta\sqrt{2}}{r}. \tag{SM:2.17}$$

Noting that

$$\int_0^{\infty}\frac{e^{-\zeta}d\zeta}{\cosh\zeta}\sin(\beta\zeta)=\frac{1}{\beta}\left[1-\frac{\pi\beta/2}{\sinh(\pi\beta/2)}\right], \tag{SM:2.18}$$

the following result is obtained:

$$\int_0^{2\pi}\frac{d\theta}{2\pi}(1+a\cos\theta)\frac{e^{-|\zeta|}\mathrm{sgn}\zeta}{\cosh\zeta}\simeq-\frac{2a}{\pi}\cos\theta_c\sin\frac{\Delta\theta}{2}\left[1-\frac{\pi\xi_0/r\sqrt{2}}{\sinh(\pi\xi_0/r\sqrt{2})}\right]. \tag{SM:2.19}$$

Substituting Eqs. (SM:2.13), (SM:2.16) and (SM:2.19) into Eq. (SM:2.5) shows that the equation $\langle\mu\rangle_{\mathrm{interface}}=0$ can be reduced to:

$$\left[\left(\frac{r\phi_0}{\xi_0}\right)^2(1-\mathcal{S})+\frac{1}{3}\mathcal{S}\right]\cos\theta_c\sin\frac{\Delta\theta}{2}-\frac{r\phi_0\sqrt{2}}{a\xi_0}\left(1+a\cos\theta_c\cos\frac{\Delta\theta}{2}\mathcal{S}\right)=0, \tag{SM:2.20}$$

where $\mathcal{S}=(\pi\xi_0/r\sqrt{2})/\sinh(\pi\xi_0/r\sqrt{2})$. The above equation is quadratic with respect to ϕ_0. Its solution can be expanded with respect to ξ_0, yielding the leading order contribution:

$$\phi_0=\frac{\xi_0}{3R\sqrt{2}}\frac{\cos\theta_c\sin(\Delta\theta/2)}{1+a\cos\theta_c\cos(\Delta\theta/2)}, \tag{SM:2.21}$$

where a term of order $O(\xi_0^3)$ was neglected. Substituting the expression Eq. (SM:2.21) for ϕ_0 into Eq. (SM:2.2) yields Eq. (6.27) in the main text.

SM:2.2. *Conservation of stripe area*

As discussed in Sec. 6 of the main text, in a multicomponent fluid with immiscible components, it is natural to expect that the area of a stripe of the minority component embedded in the majority component is conserved. The purpose of this section is to establish that this is indeed the case in the Cahn-Hilliard model employed in this paper for the fluid stripe on the torus. Starting with the hyperbolic profile given in Eq. (SM:2.1), let Φ_{tot} be the integral of ϕ over the whole torus:

$$\Phi_{\mathrm{tot}}=2\pi rR\int_0^{2\pi}d\theta(1+a\cos\theta)\phi. \tag{SM:2.22}$$

Noting that ϕ_0 is a constant and employing Eq. (SM:2.6) to replace $\tanh\zeta$ yields:

$$\begin{aligned}\Phi_{\mathrm{tot}}=&A_{\mathrm{total}}\left(\phi_0+\Phi_{\mathrm{bulk}}+\Phi_{\mathrm{interface}}\right),\\ \Phi_{\mathrm{bulk}}=&\int_0^{2\pi}\frac{d\theta}{2\pi}(1+a\cos\theta)\mathrm{sgn}\zeta,\\ \Phi_{\mathrm{interface}}=&-\int_0^{2\pi}\frac{d\theta}{2\pi}(1+a\cos\theta)\frac{e^{-|\zeta|}\mathrm{sgn}\zeta}{\cosh\zeta}.\end{aligned} \tag{SM:2.23}$$

Using Eqs. (SM:2.8) and (SM:2.19) to evaluate the integrals in the bulk and interface terms, Φ_{bulk} and $\Phi_{\mathrm{interface}}$, yields:

$$\frac{\Phi_{\mathrm{tot}}}{A_{\mathrm{total}}}=1-\frac{2\Delta A}{A_{\mathrm{total}}}+\phi_0+\frac{2a}{\pi}\cos\theta_c\sin\frac{\Delta\theta}{2}(1-\mathcal{S}), \tag{SM:2.24}$$

where $\mathcal{S} = (\pi\xi_0/r\sqrt{2})/\sinh(\pi\xi_0/r\sqrt{2})$.

Noting that $d\Phi_{\rm tot}/dt = 0$ by virtue of the Cahn-Hilliard equation (Eq. (2.12) in the paper), it can be seen that ΔA is conserved up to $O(\xi_0)$ throughout the evolution. In particular, taking the differential of Eq. (SM:2.24) gives:

$$d\frac{\Delta\theta}{2} = d\theta_c \frac{a\sin\theta_c \sin(\Delta\theta/2)}{1 + a\cos\theta_c\cos(\Delta\theta/2)} \left[1 - \frac{\pi\xi_0}{6r\sqrt{2}} \frac{1 - a^2\cos^2\theta_c}{[1 + a\cos\theta_c\cos(\Delta\theta/2)]^3} + O(\xi_0^2)\right]. \tag{SM:2.25}$$

The second term in the square bracket represents an interface correction to the relation given in Eq. (6.5) of the paper. This correction is typically below 1% so we ignore it everywhere outside this section.

SM:2.3. *Minimisation of free energy*

We now consider the problem of establishing the minimisation criterion for the free energy of the stripe configuration.

The free energy Ψ, introduced in Eq. (2.6) of the main text, is given for an azimuthally symmetric configuration on the torus by:

$$\Psi = \frac{\pi}{2} rRA \int_0^{2\pi} d\theta (1 + a\cos\theta) \left[(1-\phi^2)^2 + \frac{2\xi_0^2}{r^2}\left(\frac{\partial\phi}{\partial\theta}\right)^2\right], \tag{SM:2.26}$$

where the relation $\kappa = \xi_0^2 \mathrm{A}$ was used in the second term. Inserting the hyperbolic tangent profile, Eq. (SM:2.1), in the above expression allows Ψ to be split into two contributions, $\Psi_{\rm bulk}$ and $\Psi_{\rm interface}$, as follows:

$$\begin{aligned}
\Psi =& \Psi_{\rm bulk} + \Psi_{\rm interface},\\
\Psi_{\rm bulk} =& \frac{A_{\rm total}A}{4}\int_0^{2\pi}\frac{d\theta}{2\pi}(1+a\cos\theta)(4\phi_0^2 + 4\phi_0^3 \mathrm{sgn}\zeta + \phi_0^4),\\
\Psi_{\rm interface} =& \frac{A_{\rm total}A}{2}\int_0^{2\pi}\frac{d\theta}{2\pi}(1+a\cos\theta)\left(\frac{1}{\cosh^4\zeta} - \frac{2\phi_0\tanh\zeta + 3\phi_0^2}{\cosh^2\zeta} - \frac{2\phi_0^3\mathrm{sgn}\zeta e^{-|\zeta|}}{\cosh\zeta}\right),
\end{aligned} \tag{SM:2.27}$$

where the relation $(2\xi_0^2/r^2)(\partial_\theta\phi)^2 = 1/\cosh^4\zeta$ was employed. It should be noted that the split into bulk and interface contributions is not identical to the split with respect to the bulk and gradient free energy densities, given in Eq. (2.6).

The term $\Psi_{\rm bulk}$ can be evaluated using Eqs. (SM:2.7) and (SM:2.8):

$$\Psi_{\rm bulk} = \frac{A_{\rm total}A}{4}\phi_0^2\left[4 + \phi_0^2 + 4\phi_0\left(1 - \frac{2\Delta A}{A_{\rm total}}\right)\right]. \tag{SM:2.28}$$

Since ϕ_0, computed in Eq. (SM:2.21), is of order ξ_0, it is clear that $\Psi_{\rm bulk}$ contributes terms of order $O(\xi_0^2)$ to Ψ.

When evaluating the interface term, $\Psi_{\rm interface}$, the relation in Eq. (SM:2.10) can be employed to eliminate the term proportional to $\tanh\zeta/\cosh^2\zeta$ from Eq. (SM:2.27):

$$\Psi_{\rm interface} = \frac{A_{\rm total}A}{2}\int_0^{2\pi}\frac{d\theta}{2\pi}(1+a\cos\theta)\left(\frac{1}{\cosh^4\zeta} + \frac{3\phi_0^2}{\cosh^2\zeta} + \frac{4\phi_0^3\mathrm{sgn}\zeta e^{-|\zeta|}}{\cosh\zeta}\right). \tag{SM:2.29}$$

Looking at Eqs. (SM:2.13) and (SM:2.19), it is clear that the last two terms above make contributions of orders $O(\xi_0^3)$ and $O(\xi_0^5)$, respectively. Thus, the leading contribution

comes from the first term, which can be evaluated by noting that:

$$\int_0^{2\pi} \frac{d\theta}{2\pi}(1+a\cos\theta)\frac{1}{\cosh^4\zeta} = \frac{4\xi_0\sqrt{2}}{3\pi r}\left[1+a\cos\theta_c\cos\frac{\Delta\theta}{2}\left(1+\frac{\xi_0^2}{2r^2}\right)\frac{\pi\xi_0/r\sqrt{2}}{\sinh(\pi\xi_0/r\sqrt{2})}\right]. \tag{SM:2.30}$$

The result above was obtained using the same techniques employed in deriving the result in Eq. (SM:2.13), together with the following identities:

$$\int_0^\infty \frac{d\zeta}{\cosh^4\zeta} = \frac{2}{3}, \qquad \int_0^\infty \frac{d\zeta}{\cosh^4\zeta}\cos(\beta\zeta) = \frac{2}{3}\left(1+\frac{\beta^2}{4}\right)\frac{\pi\beta/2}{\sinh(\pi\beta/2)}. \tag{SM:2.31}$$

Using Eq. (SM:2.30), it can be shown that

$$\Psi_{\text{interface}} = \frac{\sigma A_{\text{total}}}{\pi r}\left(1+a\cos\theta_c\cos\frac{\Delta\theta}{2}\right)+O(\xi_0^3), \tag{SM:2.32}$$

where σ is the line tension on the flat geometry $\sigma=\sqrt{\frac{8\kappa \mathrm{A}}{9}}$. The term in the parenthesis can be expressed in terms of the total length of the stripe interface, ℓ_{total}, derived in Eq. (6.3) of the paper. Keeping in mind that Ψ_{bulk} is of order $O(\xi_0^2)$, the total free energy can be expressed as:

$$\Psi = \sigma\ell_{\text{total}} + O(\xi_0^2). \tag{SM:2.33}$$

SM:2.4. *Diffusive Dynamics*

In this section, we are interested in analysing the dynamics of axisymmetric stripes in the absence of hydrodynamics. That is, we consider that the evolution of the order parameter ϕ is governed by the Cahn-Hilliard equation without the advection term (setting $u^{\hat{\imath}}=0$):

$$\partial_t\phi = M\Delta\mu, \qquad \Delta\mu = \frac{1}{r^2(1+a\cos\theta)}\frac{\partial}{\partial\theta}\left[(1+a\cos\theta)\frac{\partial\mu}{\partial\theta}\right]. \tag{SM:2.34}$$

The connection between the Cahn-Hilliard equation reproduced above and the evolution of the stripe centre θ_c can be made by evaluating the former on the stripe interfaces, i.e. where $\theta=\theta_\pm$ (we refer the reader to Sec. 6 of the paper for more details on the notation used in this section). It is clear that a quantitative analysis of the features of the diffusive dynamics requires a precise knowledge of the interface details, which is beyond the scope of the current work. Instead, we focus on the hyperbolic tangent model introduced in Eq. (SM:2.1). The time derivative of ϕ evaluated on the two interfaces is:

$$\left.\frac{\partial\phi}{\partial t}\right]_{\theta_\pm} = \dot{\phi}_0 \mp \frac{r\dot{\theta}_\pm}{\xi_0\sqrt{2}}, \tag{SM:2.35}$$

where the time dependence of ϕ_0 comes through θ_c and $\Delta\theta$ in Eq. (SM:2.21). Noting that $\theta_\pm=\theta_c\pm(\Delta\theta/2)$, the time evolution of θ_c can be analysed by subtracting $\partial_t\phi(\theta_-)$ and $\partial_t\phi(\theta_+)$:

$$\dot{\theta}_c \simeq \frac{\xi_0 M}{r\sqrt{2}}\left[(\Delta\mu)_- - (\Delta\mu)_+\right]. \tag{SM:2.36}$$

Considering the split $\mu=\mu_{\text{b}}+\mu_{\text{g}}$ given in Eq. (2.9) of the main text, where

$$\mu_{\text{b}} = -A\phi(1-\phi^2), \qquad \mu_{\text{g}} = -\frac{A\xi_0^2}{r^2}\left[\frac{\partial^2\phi}{\partial\theta^2} - \frac{a\sin\theta}{1+a\cos\theta}\frac{\partial\phi}{\partial\theta}\right], \tag{SM:2.37}$$

the Laplacian $(\Delta\mu)_\pm = (\Delta\mu_{\rm b})_\pm + (\Delta\mu_{\rm g})_\pm$ on the right hand side of Eq. (SM:2.36) can be evaluated by noting that:

$$\Delta\mu_{\rm b} = -\frac{A}{r^2}\left[\left(\frac{\partial^2\phi}{\partial\theta^2} - \frac{a\sin\theta}{1+a\cos\theta}\frac{\partial\phi}{\partial\theta}\right)(1-3\phi^2) - 6\phi\left(\frac{\partial\phi}{\partial\theta}\right)^2\right],$$
$$\Delta\mu_{\rm g} = -\frac{A\xi_0^2}{r^4}\left[\frac{\partial^4\phi}{\partial\theta^4} - \frac{2a\sin\theta}{1+a\cos\theta}\frac{\partial^3\phi}{\partial\theta^3} - \left[1-\frac{1-a^2}{(1+a\cos\theta)^2}\right]\frac{\partial^2\phi}{\partial\theta^2} + \frac{a(1-a^2)\sin\theta}{(1+a\cos\theta)^3}\frac{\partial\phi}{\partial\theta}\right]. \tag{SM:2.38}$$

In order to assess the evolution of the stripe configuration, the following relations are useful:

$$\phi(\theta_\pm) = \phi_0, \qquad \left.\frac{\partial\phi}{\partial\theta}\right|_{\theta_\pm} = \pm\frac{r}{\xi_0\sqrt{2}}, \qquad \left.\frac{\partial^2\phi}{\partial\theta^2}\right|_{\theta_\pm} = 0,$$
$$\left.\frac{\partial^3\phi}{\partial\theta^3}\right|_{\theta_\pm} = \mp\frac{r^3}{\xi_0^3\sqrt{2}}, \qquad \left.\frac{\partial^4\phi}{\partial\theta^4}\right|_{\theta_\pm} = 0. \tag{SM:2.39}$$

It can be shown that:

$$(\Delta\mu)_\pm = -\frac{A}{r^2}\left[\pm\frac{r}{\xi_0\sqrt{2}}\frac{a\sin\theta_\pm}{1+a\cos\theta_\pm} - \frac{3\phi_0 r^2}{\xi_0^2} + O(\xi_0)\right]. \tag{SM:2.40}$$

Neglecting the $O(\xi_0)$ term, Eq. (SM:2.36) becomes:

$$\dot\theta_c - \frac{AM}{rR}\frac{\sin\theta_c[\cos(\Delta\theta/2) + a\cos\theta_c]}{(1+a\cos\theta_-)(1+a\cos\theta_+)} = 0. \tag{SM:2.41}$$

It can be seen that the above equation governs the relaxation of θ_c towards the equilibrium position, as given by Eq. (6.7) of the main text. In order to assess the dynamics of this approach to equilibrium, it is convenient to introduce the notation:

$$\theta_c = \theta_c^{eq} + \delta\theta, \tag{SM:2.42}$$

where θ_c^{eq} is the expected equilibrium position. For small departures $\delta\theta = \theta - \theta_c^{eq}$, Eqs. (7.15) and (7.16) can be used to replace the second term in Eq. (SM:2.41) via:

$$\frac{\sin\theta_c\left(a\cos\theta_c + \cos\frac{\Delta\theta}{2}\right)}{(1+a\cos\theta_+)(1+a\cos\theta_-)} \simeq -\delta\theta\begin{cases}\dfrac{\cos(\Delta\theta_{eq}/2)-a}{[1-a\cos(\Delta\theta_{eq}/2)]^2}, & \Delta A < \Delta A_{\rm crit},\\ \dfrac{2a\sin^2\theta_c^{eq}}{(1-a^2)\sin^2(\Delta\theta_{eq}/2)}, & \Delta A > \Delta A_{\rm crit}.\end{cases} \tag{SM:2.43}$$

such that the solution of this equation takes the form:

$$\delta\theta = \delta\theta_0 e^{-2\alpha_\mu t}, \tag{SM:2.44}$$

where $\delta\theta_0$ is an integration constant, while α_μ is given by:

$$\alpha_\mu = \begin{cases}\dfrac{AM}{2r^2}\dfrac{a(\cos(\Delta\theta_{eq}/2)-a)}{[1-a\cos(\Delta\theta_{eq}/2)]^2}, & \Delta A < \Delta A_{\rm crit},\\ \dfrac{2AMa^2}{r^2(1-a^2)}\dfrac{\sin^2\theta_c^{eq}}{\sin^2(\Delta\theta_{eq}/2)}, & \Delta A > \Delta A_{\rm crit}.\end{cases} \tag{SM:2.45}$$

The analysis presented up until now reveals the essential features of the drift of stripe configurations, in the absence of hydrodynamics. Eq. (SM:2.41) predicts that the stripes approach their equilibrium position exponentially.

These features are confirmed by our numerical simulations. Figure SM:1 shows the

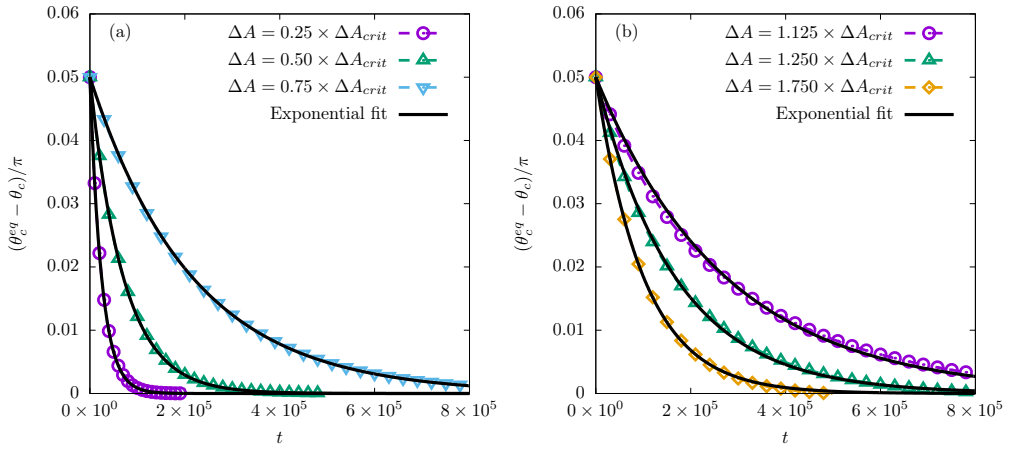

Figure SM:1. Time evolution of $(\theta_c^{eq} - \theta_c)/\pi$ for (a) stripes with areas $\Delta A < \Delta A_{\rm crit}$ (equilibrating at $\theta_c^{eq} = \pi$); and (b) stripes with areas $\Delta A > \Delta A_{\rm crit}$ (equilibrating at $\theta_c^{eq} < \pi$), as shown in Table 1. The dotted lines with points are obtained by fitting Eq. (SM:2.1) to the numerical data with ϕ_0, ξ_0, θ_c and $\Delta\theta$ as free parameters. The solid lines are obtained by fitting Eq. (SM:2.47) to the numerical curves with $\alpha_{\mu;\rm emp}$ as a free parameter, while $\delta\theta_0 = \pi/20$. The values of $\alpha_{\mu;\rm emp}$ are reported in Table 1.

$\Delta A/\Delta A_{\rm crit}$	$\Delta\theta_{eq}/\pi$	θ_c^{eq}/π	α_μ [Eq. (SM:2.45)]	$\alpha_{\mu;\rm emp}$ [Eq. (SM:2.48)]	$F(\Delta\theta_{eq}; a)$
0.25	0.208	1	5.54×10^{-4}	2.03×10^{-5}	2.46
0.5	0.403	1	3.46×10^{-4}	7.10×10^{-6}	1.38
0.75	0.580	1	1.46×10^{-4}	2.32×10^{-6}	1.06
1.125	0.775	0.834	2.11×10^{-4}	1.83×10^{-6}	0.581
1.25	0.810	0.763	3.74×10^{-4}	2.99×10^{-6}	0.537
1.75	0.941	0.574	7.11×10^{-4}	4.97×10^{-6}	0.469

Table 1. Numerical values for the ratio $\Delta A/\Delta A_{\rm crit}$ of the stripe area to the critical area; of the corresponding stripe width $\Delta\theta_{eq}$ at equilibrium (in units of π); of the equilibrium position (in units of π); of the damping coefficient α_μ predicted through Eq. (SM:2.45); of the damping coefficient $\alpha_{\mu;\rm emp}$ obtained by fitting Eq. (SM:2.47) to the numerical data; and of the coefficient $F(\Delta\theta_{eq}; a)$ entering in the empirical expression, Eq. (SM:2.48). The torus parameters are $r = 0.8$ and $R = 2$, such that $a = 0.4$.

approach to equilibrium for stripes having various areas ΔA compared to the critical area $\Delta A_{\rm crit}$, on a torus with $r = 0.8$ and $R = 2$ ($a = 0.4$). The mobility was set to $M = 2.5 \times 10^{-3}$, while $A = 0.5$ and $\kappa = 5 \times 10^{-4}$. While the equilibrium position corresponds to the one predicted via Eq. (SM:2.41), the damping coefficient α_μ given in Eq. (SM:2.45) is between one and two orders of magnitude larger than the one observed numerically, as can be seen from Table 1. This discrepancy could be attributed to the fact that some of the assumptions made in this section are not strictly valid in the present context.

On the torus geometry, the Laplace-Beltrami operator appearing in μ_κ contains a term involving a first order derivative of ϕ, as can be seen in Eq. (SM:2.37). When the stripe is in equilibrium (i.e., when the stationary state is achieved), the solution of the equation

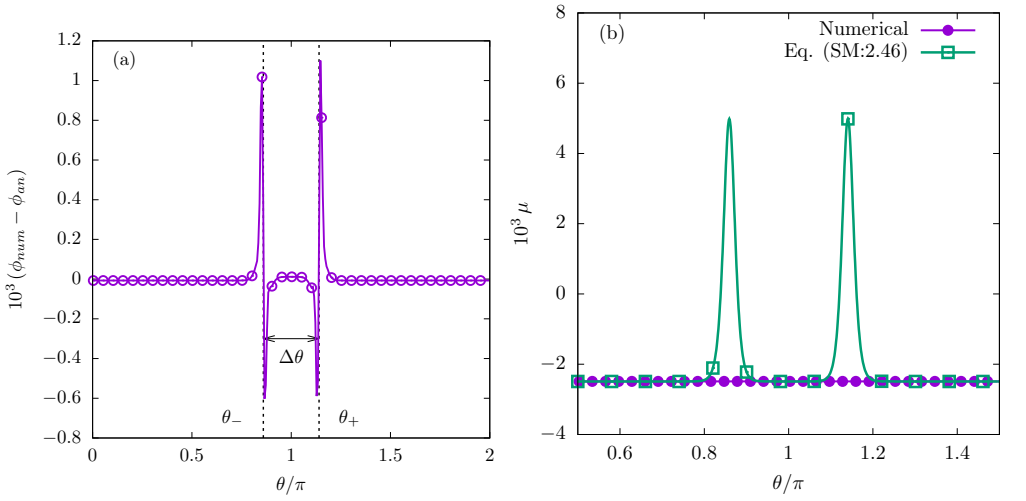

Figure SM:2. (a) The difference between the numerical profile $\phi_{\rm num}$ of the order parameter and the hyperbolic tangent approximation given in Eq. (SM:2.1); (b) Comparison between the numerical profile for the chemical potential μ and the approximation given by Eq. (SM:2.46). These configurations are represented at $t = 20\,000$ for a stripe initialised using Eq. (SM:2.1) with $\theta_c = \pi$ and $\Delta\theta = 0.280406\pi$. The simulation parameters are $\kappa = 5 \times 10^{-4}$, $A = 0.5$, $M = 2.5 \times 10^{-3}$, $r = 0.8$ and $R = 2$.

$\Delta\mu = 0$ is $\mu = \mu_0 = \text{const}$, with $\mu_0 = 2A\phi_0$, as discussed in Eq. (SM:2.4). Introducing the hyperbolic tangent profile, Eq. (SM:2.1), yields:

$$\mu = 2A\phi_0 - \frac{3A}{\cosh^2\zeta}\left[\phi_0 - \text{sgn}(\theta-\theta_c)\frac{\xi_0}{3r\sqrt{2}}\frac{a\sin\theta}{1+a\cos\theta}\right] + O(\xi_0^2). \qquad \text{(SM:2.46)}$$

Thus, it can be seen that the chemical potential presents variations in the vicinity of the interface when the order parameter profile is approximated using a hyperbolic tangent. Figure SM:2(a) shows the difference $\phi_{\rm num} - \phi_{\rm an}$ between the profile of the order parameter obtained numerically and the analytic formula, Eq. (SM:2.1), for a stripe located at $\theta_c^{eq} = \pi$ with $\Delta\theta = 0.280406\pi$. It can be seen that the order parameter presents very small deviations from Eq. (SM:2.1) in the vicinity of the interfaces. Figure SM:2(b) shows the chemical potential obtained from the numerical simulation compared with the analytic expression, Eq. (SM:2.46). Even though the stripe is in equilibrium, Eq. (SM:2.46) predicts variations around the interfaces. Eliminating the term in the parenthesis on the right hand side of Eq. (SM:2.46) is the key to understanding the leading order term in the problem of diffusive dynamics, however we do not further pursue this analysis here and leave this avenue of research for future work.

The above discussion prompts us to look for an empirical expression $\alpha_{\mu;\text{emp}}$ for the damping coefficient. We first check the dependence of $\alpha_{\mu;\text{emp}}$ on the mobility M and surface tension σ by fitting Eq. (SM:2.44) to the numerical results for the time evolution of the stripe centre obtained through various simulations. In the first batch of simulations, the ratio $a = r/R$ is fixed at $a = 0.4$, while r takes the values 0.8, 1.0 and 1.2. Keeping $\kappa = 5 \times 10^{-4}$ and $A = 0.5$ fixed, Figs. SM:3(a) and SM:3(b), corresponding to $\theta_c^{eq} = \pi$ ($\Delta\theta_{eq} = 0.283\pi$) and $\theta_c^{eq} = 3\pi/4$ ($\Delta\theta_{eq} = 0.817\pi$), respectively, indicate a clear linear dependence of $\alpha_{\mu;\text{emp}}$ with respect to the mobility parameter, M. In order to ensure that the grid spacing does not exceed the interface width $\xi_0 = \sqrt{\kappa/A} \simeq 0.0316$, the number of nodes is taken to be $N_\theta = 320$ ($r = 0.8$), 400 ($r = 1.0$) and 480 ($r = 1.2$). The time step

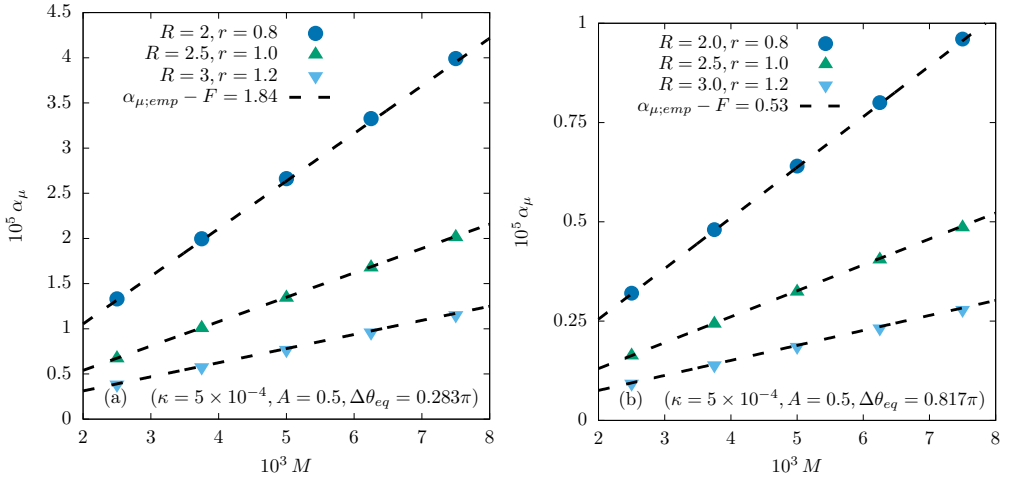

Figure SM:3. Damping coefficient $\alpha_{\mu;\mathrm{emp}}$ with respect to M for $r = 0.8$, 1.0 and 1.2 at fixed $a = r/R = 0.4$, obtained by fitting Eq. (SM:2.44) to the simulation results (points). The dashed lines represent the best linear fit of the data. The results correspond to stripes having (a) $\Delta\theta_{eq} \simeq 0.283\pi$ ($\theta_c^{eq} = \pi$); and (b) $\Delta\theta_{eq} \simeq 0.8174\pi$ ($\theta_c^{eq} = 3\pi/4$).

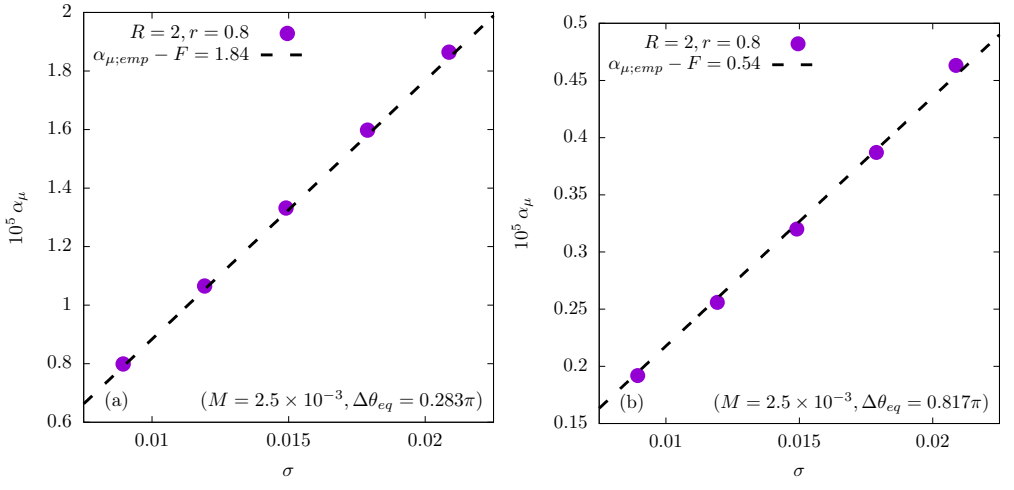

Figure SM:4. Damping coefficient $\alpha_{\mu;\mathrm{emp}}$ with respect to $\sigma = \sqrt{8\kappa A/9}$ for $r = 0.8$, $a = 0.4$ and fixed $\xi_0 = \sqrt{\kappa/A} \simeq 0.0316$, obtained by fitting Eq. (SM:2.44) to the simulation results (points). The dashed lines represent the best linear fit of the data. The results correspond to stripes having (a) $\Delta\theta_{eq} \simeq 0.283\pi$ ($\theta_c^{eq} = \pi$); and (b) $\Delta\theta_{eq} \simeq 0.817\pi$ ($\theta_c^{eq} = 3\pi/4$).

is taken to be $\delta t = 10^{-3}$ in order to prevent the Cahn-Hilliard equation from becoming stiff.

In the second batch of simulations, the dependence of $\alpha_{\mu;\mathrm{emp}}$ on the surface tension $\sigma = \sqrt{\frac{8\kappa A}{9}}$ is examined. Keeping $r = 0.8$ ($N_\theta = 320$), $a = 0.4$ and $M = 2.5 \times 10^{-3}$ fixed, κ and A are varied such that the interface width $\xi_0 = \sqrt{\frac{\kappa}{A}} \simeq 0.0316$ is kept constant. The time step is $\delta t = 2.5 \times 10^{-3}$ for all simulations. It can be seen in Figs. SM:4(a) and SM:4(b), corresponding to $\theta_c^{eq} = \pi$ and $\theta_c^{eq} = 3\pi/4$, respectively, that $\alpha_{\mu;\mathrm{emp}}$ presents a linear dependence on σ. This results is in contradiction to Eq. (SM:2.45).

Based on the above analysis, Eqs. (SM:2.41) and (SM:2.44) can be written as:

$$\dot{\delta\theta} + 2\alpha_{\mu;\mathrm{emp}}\delta\theta = 0, \qquad \delta\theta = \delta\theta_0 e^{-2\alpha_{\mu;\mathrm{emp}}t}, \tag{SM:2.47}$$

where an empirical formula $\alpha_{\mu;\mathrm{emp}}$ can be proposed by multiplying Eq. (SM:2.45) with $a\sigma F(\Delta\theta_{eq}, a)/Ar$:

$$\alpha_{\mu;\mathrm{emp}} = \begin{cases} \dfrac{a\sigma M}{2r^3}\dfrac{a[\cos(\Delta\theta_{eq}/2) - a]}{[1 - a\cos(\Delta\theta_{eq}/2)]^2} \times F(\Delta\theta_{eq}, a), & \Delta A < \Delta A_{\mathrm{crit}}, \\ \dfrac{2a^3\sigma M}{r^3(1-a^2)}\dfrac{\sin^2\theta_c^{eq}}{\sin^2(\Delta\theta_{eq}/2)} \times F(\Delta\theta_{eq}, a), & \Delta A > \Delta A_{\mathrm{crit}}. \end{cases} \tag{SM:2.48}$$

In the above, $F(\Delta\theta_{eq}, a)$ is an unknown function that can depend (up to first order with respect to ξ_0) only on the stripe width at equilibrium ($\Delta\theta_{eq}$) and on the ratio $a = r/R$ of the torus radii. Fitting the expression to the numerical data corresponding to Fig. SM:3 gives $F(0.283\pi, 0.4) \simeq 1.84$ and $F(0.817\pi, 0.4) \simeq 0.53$. Further values corresponding to the stripes considered in Fig. SM:1 are summarised in Table 1.

We now turn our attention to another interesting aspect of the empirical formula, Eq. (SM:2.48). It can be seen that the damping coefficient is expected to vanish on both branches for critical stripes, when $\theta_c^{eq} = \pi$ and $\Delta\theta_{eq} = 2\arccos a$. The fact that $\alpha_{\mu;\mathrm{emp}}$ vanishes when $\Delta A = \Delta A_{\mathrm{crit}}$ is related to the presence of the term $\sin\theta_c[a\cos\theta_c + \cos(\Delta\theta/2)]$ in the numerator of Eq. (SM:2.41). When $\alpha_{\mu;\mathrm{emp}}$ is negligible, the higher order terms in the expansion of $\sin\theta_c[a\cos\theta_c + \cos(\Delta\theta/2)]$ dominate the evolution of the stripe towards its equilibrium position. It can already be seen in Fig. SM:1(b) that at $\Delta A = 1.125\Delta A_{\mathrm{crit}}$, the exponentially decaying solution presents some discrepancy with respect to the numerical simulation. In order to explain this discrepancy, we reconsider Eq. (SM:2.48) by including the next-to-leading order term with respect to $\delta\theta$.

For close to critical stripes, centred at a distance $\delta\theta = \theta_c - \theta_c^{eq}$ away from their equilibrium position at $\theta_c^{eq} = \pi$, the width $\Delta\theta$ can be found by imposing that their area, $\Delta A = 2\pi r R[\Delta\theta + 2a\sin(\Delta\theta/2)\cos\theta_c]$, remains constant:

$$\Delta\theta = \Delta\theta_{eq} - \frac{a\sin(\Delta\theta_{eq}/2)}{1 - a\cos(\Delta\theta_{eq})}\delta\theta^2 + O(\delta\theta^4). \tag{SM:2.49}$$

Considering that the difference $\delta\Delta\theta_{eq} = 2\arccos a - \Delta\theta_{eq}$ between the critical width $2\arccos a$ and the stripe width is small, Eq. (SM:2.41) reduces to:

$$\dot{\delta\theta} + 2\alpha_{\mu;\mathrm{emp}}\delta\theta + \alpha^{(3)}_{\mu;\mathrm{emp}}\delta\theta^3 = 0, \tag{SM:2.50}$$

where

$$\begin{aligned} \alpha_{\mu;\mathrm{emp}} =& \frac{a\sigma M}{2r^3}\frac{a[\cos(\Delta\theta_{eq}/2) - a]}{[1 - a\cos(\Delta\theta_{eq}/2)]^2}F(\Delta\theta_{eq}, a) \simeq \frac{a\sigma M}{2r^3}\frac{a\delta\Delta\theta_{eq}}{2(1-a^2)^{3/2}}F_{\mathrm{crit}}, \\ \alpha^{(3)}_{\mu;\mathrm{emp}} \simeq& \frac{a\sigma M}{2r^3}\frac{2a^2}{(1-a^2)^2}F_{\mathrm{crit}}\left[1 + O(\delta\Delta\theta_{eq})\right], \end{aligned} \tag{SM:2.51}$$

where $F_{\mathrm{crit}} \equiv F(\Delta\theta_{eq}^{\mathrm{crit}}, a)$ and $\Delta\theta_{eq}^{\mathrm{crit}} = 2\arccos a$. The solution of Eq. (SM:2.50) is

$$\delta\theta = \delta\theta_0 e^{-2\alpha_{\mu;\mathrm{emp}}t}\left[1 + \frac{\alpha^{(3)}_{\mu;\mathrm{emp}}}{2\alpha_{\mu;\mathrm{emp}}}\delta\theta_0^2(1 - e^{-4\alpha_{\mu;\mathrm{emp}}t})\right]^{-1/2}. \tag{SM:2.52}$$

In the limit of the critical stripe, $\alpha_{\mu;\mathrm{emp;crit}} = 0$ and the above equation reduces to:

$$\delta\theta_{\mathrm{crit}} = \delta\theta_0\left[1 + 2\alpha^{(3)}_{\mu;\mathrm{emp}}\delta\theta_0^2 t\right]^{-1/2}. \tag{SM:2.53}$$

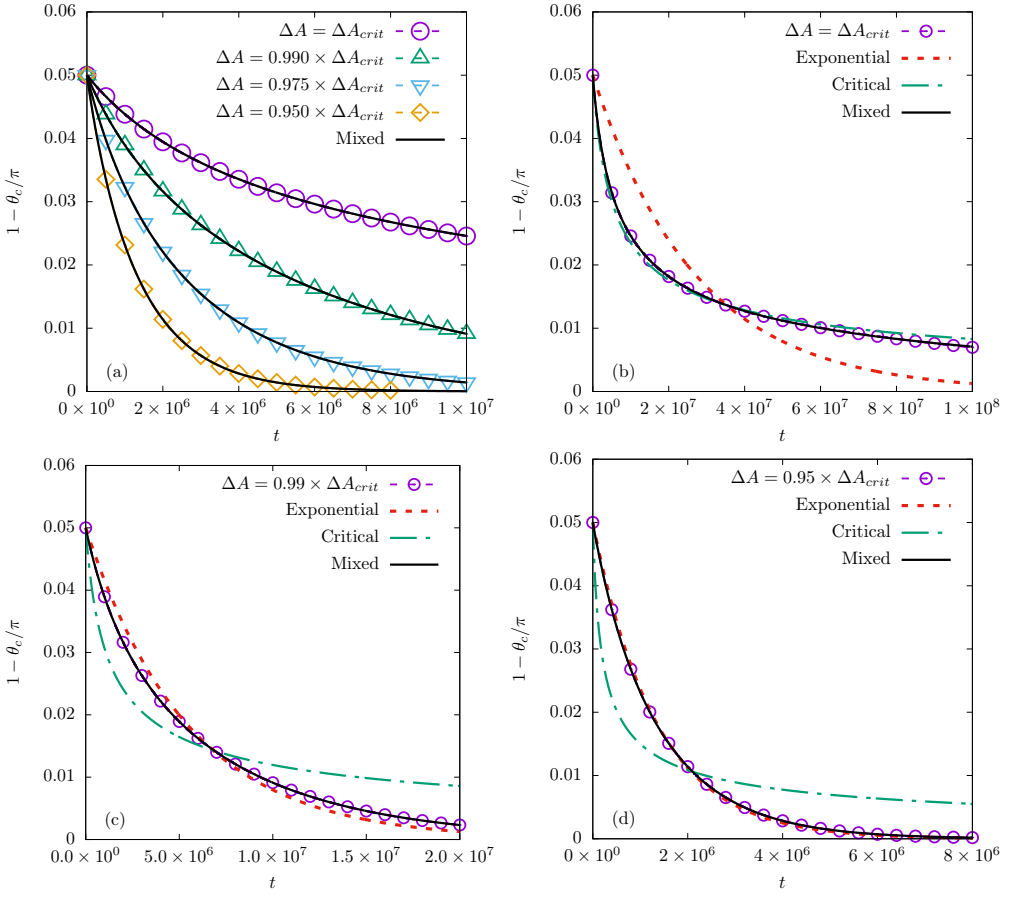

Figure SM:5. Comparison between numerical results (dotted lines and points) and various fitting formulae for the time evolution of $1-\theta_c/\pi$ for stripes with various areas ΔA. (a) Comparison with the mixed solution in Eq. (SM:2.52), where $\alpha_{\mu;\mathrm{emp}}$ and $\alpha^{(3)}_{\mu;\mathrm{emp}}$ are free parameters (shown with solid black lines); (b)–(d) Best fit curves corresponding to: the exponential solution in Eq. (SM:2.48) with $\alpha_{\mu;\mathrm{emp}}$ as a free parameter (dotted lines); the critical solution in Eq. (SM:2.53) with $\alpha^{(3)}_{\mu;\mathrm{emp}}$ as a free parameter (dash-dotted lines); and the mixed solution, fitted as for (a). The initial amplitude is always $\delta\theta_0 = -\pi/20$, expressed with respect to the equilibrium position $\theta_c^{eq} = \pi$.

In order to validate the above analysis, the exponential (Eq. (SM:2.48)); critical (Eq. (SM:2.53)); and mixed (Eq. (SM:2.52)) functional forms are fitted to numerical results using $\alpha_{\mu;\mathrm{emp}}$; $\alpha^{(3)}_{\mu;\mathrm{emp}}$; and $\alpha_{\mu;\mathrm{emp}}$ and $\alpha^{(3)}_{\mu;\mathrm{emp}}$ as free parameters, respectively. The initial amplitude is set to $\delta\theta_0 = -\pi/20$. Figure SM:5(a) shows the evolution of the stripe centres for stripes having areas ΔA equal to ΔA_{crit} (critical stripe), $0.99\Delta A_{\mathrm{crit}}$, $0.975\Delta A_{\mathrm{crit}}$ and $0.95\Delta A_{\mathrm{crit}}$. The mixed solution, Eq. (SM:2.52), shown with continuous black lines, is fitted to the numerical results (shown with dotted lines and points), using $\alpha_{\mu;\mathrm{emp}}$ and $\alpha^{(3)}_{\mu;\mathrm{emp}}$ as free parameters. An excellent agreement can be seen in all cases and the value for F obtained by comparing the fitted values with the analytic expressions (Eq. (SM:2.51)) is around $F \simeq 0.93$. Figures SM:5(b)–SM:5(d) present comparisons between the numerical results corresponding to three stripe areas and the exponential (Eq. (SM:2.48)), critical (Eq. (SM:2.53)) and mixed (Eq. (SM:2.52)) solutions, fitted to

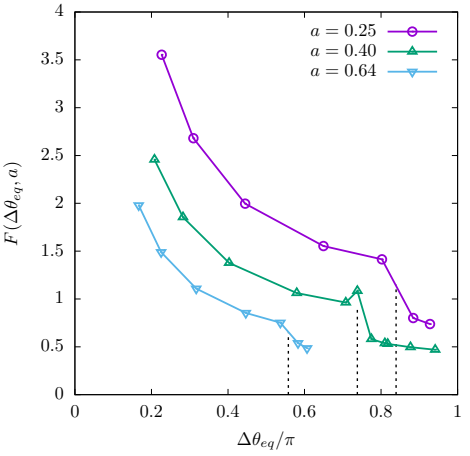

Figure SM:6. Dependence of the factor $F(\Delta\theta_{eq}, a)$ on $\Delta\theta_{eq}/\pi$ for various values of a. It can be seen that $F(\Delta\theta_{eq}, a)$ is discontinuous at the critical point, where $\Delta\theta_{eq} = 2\arccos a$ (this point is marked with dotted vertical lines).

the numerical results using the coefficients $\alpha_{\mu;\mathrm{emp}}$ and $\alpha^{(3)}_{\mu;\mathrm{emp}}$ as free parameters. It can be seen that for the critical stripe, shown in Fig. SM:5(b), the critical and mixed solutions are almost overlapped with the numerical results, while the exponential solution presents clear deviations. For the stripe with $\Delta A = 0.99 \times \Delta A_{\mathrm{crit}}$, neither the exponential nor the critical solutions can be used to capture the evolution of the stripe centre, while the mixed solution presents an excellent agreement with the numerical results. Finally, the evolution of the centre of the stripe with $\Delta A = 0.95 \times \Delta A_{\mathrm{crit}}$ can be seen to be well captured by the exponential solution. From this study, we conclude that the term $\sin\theta_c[a\cos\theta_c + \cos(\Delta\theta/2)]$ is indeed responsible for selecting the equilibrium position for stripe configurations.

We end with a discussion of the dependence of the function $F(\Delta\theta_{eq}, a)$ on the stripe equilibrium width $\Delta\theta_{eq}$, for three values of the torus radii ratio $a = r/R$, shown in Fig. SM:6. It can be seen that F is mostly a monotonically decreasing function of $\Delta\theta_{eq}$ and a. Also, it can be seen that there is a discontinuity in F around the critical point (where $\Delta\theta_{eq} = 2\arccos a$), which is shown using vertical dotted lines.

SM:3. Eigenfunctions on the torus

This section contains the analytical results obtained for the eigenfunctions on a torus. These functions are solutions of Eqs. (3.10) and (4.4) in the main text, in powers of the radii ratio $a = r/R$. Both equations to be solved can be conveniently written as (Eq. (B 1) of the main text is reproduced below):

$$(1 + a\cos\theta)\left(\frac{\partial^2 \Psi_n}{\partial\theta^2} + \lambda_n^2 \Psi_n\right) + \alpha a \sin\theta \frac{\partial \Psi_n}{\partial\theta} = 0, \tag{SM:3.1}$$

where $\alpha = 1$ and -3 for Eqs. (3.10) and (4.4), respectively.

In the following subsections we list the results for both intermediate values of the radii ratio $0 < a < 1$ (Sec. SM:3.1), as well as for the limiting case of $a = 1$ (Sec. SM:3.2).

For the reader's convenience, these expansions are compiled in the form of gnuplot files (`funcs-inv.gpl` and `funcs-shear.gpl`) and Mathematica notebooks (`funcs_inv.nb` and `funcs_shear.nb`).

SM:3.1. *Eigenfunctions for* $0 < a < 1$

This section of the present Supplementary material contains the results obtained for the eigenfunctions on a torus by applying the perturbative procedure detailed in Appendix B of the main text. The results obtained for $1 \leqslant n \leqslant 4$ are listed including terms up to $O(a^9)$ in the following subsections, namely for f_n and g_n (corresponding to $\alpha = 1$) are shown in Subsec. SM:3.1.1, while F_n and G_n (corresponding to $\alpha = -3$) are given in Subsec. SM:3.1.2.

SM:3.1.1. *Eigenfunctions for the inviscid case*

In this subsection we list the series solutions of Eq. (SM:3.1) for the case $\alpha = 1$.

The even and odd eigenfunctions corresponding to $n = 1$ are:

$$\begin{aligned}
\frac{1}{\sqrt{2}(1+a\cos\theta)}\begin{pmatrix} f_1/N_{1;c} \\ g_1/N_{1;s}\end{pmatrix} &= \begin{pmatrix}\cos\theta \\ \sin\theta\end{pmatrix} \\
&- \frac{a}{3}\begin{pmatrix}\cos 2\theta \\ \sin 2\theta\end{pmatrix}\left[1 + \begin{pmatrix}91\\-5\end{pmatrix}\frac{a^2}{288} + \begin{pmatrix}13\,877\\-11\,125\end{pmatrix}\frac{a^4}{82\,944} + \begin{pmatrix}\frac{2\,567\,969}{23\,887\,872}\\ -\frac{3\,564\,799}{23\,887\,872}\end{pmatrix}a^6\right] \\
&+ \frac{5\,a^2}{32}\begin{pmatrix}\cos(3\theta) \\ \sin(3\theta)\end{pmatrix}\left[1 + \begin{pmatrix}827\\293\end{pmatrix}\frac{a^2}{1440} + \begin{pmatrix}\frac{31\,475}{82\,944}\\ -\frac{78\,853}{2\,073\,600}\end{pmatrix}a^4 + \begin{pmatrix}\frac{5\,727\,710\,809}{20\,901\,888\,000}\\ -\frac{510\,034\,981}{4\,180\,377\,600}\end{pmatrix}a^6\right] \\
&- \frac{11\,a^3}{144}\begin{pmatrix}\cos(4\theta) \\ \sin(4\theta)\end{pmatrix}\left[1 + \begin{pmatrix}6\,550\\3\,517\end{pmatrix}\frac{a^2}{7\,920} + \begin{pmatrix}104\,013\,923\\20\,453\,915\end{pmatrix}\frac{a^4}{159\,667\,200}\right] \\
&+ \frac{1045\,a^4}{27648}\begin{pmatrix}\cos(5\theta) \\ \sin(5\theta)\end{pmatrix}\left[1 + \begin{pmatrix}567\,883\\363\,301\end{pmatrix}\frac{a^2}{526\,680} + \begin{pmatrix}8\,367\,078\,469\\3\,047\,011\,141\end{pmatrix}\frac{a^4}{8\,494\,295\,040}\right] \\
&- \frac{6061\,a^5}{322\,560}\begin{pmatrix}\cos(6\theta) \\ \sin(6\theta)\end{pmatrix}\left[1 + \begin{pmatrix}162\,374\,671\\114\,550\,495\end{pmatrix}\frac{a^2}{122\,189\,760}\right] \\
&+ \frac{248\,501\,a^6}{26\,542\,080}\begin{pmatrix}\cos(7\theta) \\ \sin(7\theta)\end{pmatrix}\left[1 + \begin{pmatrix}\frac{3\,390\,730\,999}{2\,147\,048\,640}\\ \frac{3\,565\,202\,867}{3\,005\,868\,096}\end{pmatrix}a^2\right] \\
&- \frac{2\,733\,511\,a^7}{585\,252\,864}\begin{pmatrix}\cos(8\theta) \\ \sin(8\theta)\end{pmatrix} + \frac{194\,079\,281\,a^8}{83\,235\,962\,880}\begin{pmatrix}\cos(9\theta) \\ \sin(9\theta)\end{pmatrix} + O(a^9),
\end{aligned} \tag{SM:3.3a}$$

where the normalisation constants $N_{1;c/s}$, eigenvalues $\lambda_{1;c/s}$ and integrals $I_{c/s;0;1}$ [defined in Eq. (3.26) of the main text] are given by:

$$\begin{aligned}
\begin{pmatrix} N_{1;c} \\ N_{1;s} \end{pmatrix} =& 1 + \frac{a^2}{9} + \begin{pmatrix} 8279 \\ 5207 \end{pmatrix} \frac{a^4}{165\,888} + \begin{pmatrix} 237\,715 \\ 25\,325 \end{pmatrix} \frac{a^6}{7\,962\,624} \\
&+ \begin{pmatrix} 5\,616\,721\,535 \\ -2\,780\,766\,337 \end{pmatrix} \frac{a^8}{275\,188\,285\,440} + O(a^{10}), \\
\begin{pmatrix} \lambda_{1;c}^2 \\ \lambda_{1;s}^2 \end{pmatrix} =& 1 + \begin{pmatrix} -1 \\ 5 \end{pmatrix} \frac{a^2}{12} + \begin{pmatrix} -23 \\ 169 \end{pmatrix} \frac{5\,a^4}{3456} + \begin{pmatrix} -18\,821 \\ 152\,485 \end{pmatrix} \frac{a^6}{995\,328} \\
&+ \begin{pmatrix} 3\,603\,881 \\ 27\,745\,879 \end{pmatrix} \frac{a^8}{286\,654\,464} + O(a^{10}). \\
I_{c;0;1} =& \frac{a}{\sqrt{2}} + \frac{a^3}{9\sqrt{2}} + \frac{8\,279\,a^5}{165\,888\sqrt{2}} + \frac{237\,715\,a^7}{7\,962\,624\sqrt{2}} + O(a^9), \\
I_{s;0;1} =& \frac{1}{\sqrt{2}} - \frac{a^2}{18\sqrt{2}} + \frac{2\,615\,a^4}{165\,888\sqrt{2}} + \frac{54\,743\,a^6}{2\,654\,208\sqrt{2}} + \frac{4\,626\,289\,343\,a^8}{275\,188\,285\,440\sqrt{2}} + O(a^{10})
\end{aligned} \tag{SM:3.3b}$$

The eigenfunctions corresponding to $n = 2$ are:

$$\begin{aligned}
\frac{1}{\sqrt{2}(1 + a\cos\theta)} \begin{pmatrix} f_2/N_{2;c} \\ g_2/N_{2;s} \end{pmatrix} =& \begin{pmatrix} \cos(2\theta) \\ \sin(2\theta) \end{pmatrix} \\
&- \frac{a}{6} \begin{pmatrix} \cos(\theta) \\ \sin(\theta) \end{pmatrix} \left[1 + \begin{pmatrix} 1 \\ 31 \end{pmatrix} \frac{a^2}{45} + \begin{pmatrix} -14 \\ 4\,936 \end{pmatrix} \frac{a^4}{10\,125} + \begin{pmatrix} -121\,742 \\ 10\,927\,933 \end{pmatrix} \frac{a^6}{31\,893\,750} \right] \\
&- \frac{3a}{10} \begin{pmatrix} \cos(3\theta) \\ \sin(3\theta) \end{pmatrix} \left[1 + \frac{17}{75}a^2 + \begin{pmatrix} 15\,238 \\ 7\,363 \end{pmatrix} \frac{a^4}{118\,125} + \begin{pmatrix} 1\,948\,651 \\ -59\,999 \end{pmatrix} \frac{a^6}{21\,262\,500} \right] \\
&+ \frac{2a^2}{15} \begin{pmatrix} \cos(4\theta) \\ \sin(4\theta) \end{pmatrix} \left[1 + \frac{2993}{6300}a^2 + \begin{pmatrix} 885\,947 \\ 670\,697 \end{pmatrix} \frac{a^4}{2\,835\,000} + \begin{pmatrix} 417\,687\,269 \\ 193\,033\,919 \end{pmatrix} \frac{a^6}{1\,786\,050\,000} \right] \\
&- \frac{4\,a^3}{63} \begin{pmatrix} \cos(5\theta) \\ \sin(5\theta) \end{pmatrix} \left[1 + \frac{1739}{2400}a^2 + \begin{pmatrix} \frac{16\,841\,243}{30\,240\,000} \\ \frac{535\,009}{1\,120\,000} \end{pmatrix} a^4 \right] \\
&+ \frac{13\,a^4}{420} \begin{pmatrix} \cos(6\theta) \\ \sin(6\theta) \end{pmatrix} \left[1 + \frac{22\,799}{23\,400}a^2 + \begin{pmatrix} \frac{15\,908\,203}{18\,427\,500} \\ \frac{57\,674\,437}{73\,710\,000} \end{pmatrix} a^4 \right] \\
&- \frac{247\,a^5}{16200} \begin{pmatrix} \cos(7\theta) \\ \sin(7\theta) \end{pmatrix} \left(1 + \frac{544\,253}{444\,600}a^2 \right) + \frac{3211\,a^6}{425\,250} \begin{pmatrix} \cos(8\theta) \\ \sin(8\theta) \end{pmatrix} \left(1 + \frac{218\,667\,527}{148\,348\,200}a^2 \right) \\
&- \frac{54\,587\,a^7}{14\,553\,000} \begin{pmatrix} \cos(9\theta) \\ \sin(9\theta) \end{pmatrix} + \frac{2\,347\,241\,a^8}{1\,257\,379\,200} \begin{pmatrix} \cos(10\theta) \\ \sin(10\theta) \end{pmatrix} + O(a^9),
\end{aligned} \tag{SM:3.3c}$$

where the normalisation constants $N_{2;c/s}$, eigenvalues $\lambda_{2;c/s}$ and integrals $I_{c/s;0;2}$ are

given by:

$$\begin{aligned}
\begin{pmatrix} N_{2;c} \\ N_{2;s} \end{pmatrix} =& 1 + \frac{157\,a^2}{900} + \begin{pmatrix} 115\,979 \\ 175\,979 \end{pmatrix} \frac{a^4}{1\,620\,000} + \begin{pmatrix} 952\,559\,651 \\ 1\,808\,883\,651 \end{pmatrix} \frac{a^6}{23\,814\,000\,000} \\
&+ \begin{pmatrix} 977\,451\,802\,981 \\ 1\,939\,193\,170\,981 \end{pmatrix} \frac{a^8}{36\,741\,600\,000\,000} + O(a^{10}), \\
\begin{pmatrix} \lambda_{2;c}^2 \\ \lambda_{2;s}^2 \end{pmatrix} =& 4 + \frac{2\,a^2}{15} + \begin{pmatrix} -8 \\ 742 \end{pmatrix} \frac{a^4}{3\,375} + \begin{pmatrix} -124\,262 \\ 1\,206\,613 \end{pmatrix} \frac{a^6}{5\,315\,625} \\
&+ \begin{pmatrix} -23\,163\,359 \\ 207\,817\,741 \end{pmatrix} \frac{a^8}{956\,812\,500} + O(a^{10}), \\
I_{c;0;2} =& -\frac{a^2}{6\sqrt{2}} - \frac{59\,a^4}{1800\sqrt{2}} - \frac{120\,019\,a^6}{9\,720\,000\sqrt{2}} - \frac{2\,681\,403\,973\,a^8}{428\,652\,000\,000\sqrt{2}} + O(a^{10}), \\
I_{s;0;2} =& \frac{a}{3\sqrt{2}} - \frac{17\,a^3}{300\sqrt{2}} - \frac{316\,241\,a^5}{4\,860\,000\sqrt{2}} - \frac{12\,523\,566\,857\,a^7}{214\,326\,000\,000\sqrt{2}} + O(a^9), \qquad \text{(SM:3.3}d\text{)}
\end{aligned}$$

The eigenfunctions corresponding to $n = 3$ are:

$$\begin{aligned}
&\frac{1}{\sqrt{2}(1 + a\cos\theta)} \begin{pmatrix} f_3/N_{3;c} \\ g_3/N_{3;s} \end{pmatrix} = \begin{pmatrix} \cos(3\theta) \\ \sin(3\theta) \end{pmatrix} \\
&+ \frac{7\,a^2}{160} \begin{pmatrix} \cos(\theta) \\ \sin(\theta) \end{pmatrix} \left[1 + \begin{pmatrix} \frac{12\,767}{39\,200} \\ \frac{34\,817}{39\,200} \end{pmatrix} a^2 + \begin{pmatrix} \frac{346\,734\,761}{3\,073\,280\,000} \\ \frac{2\,408\,497\,961}{3\,073\,280\,000} \end{pmatrix} a^4 + \begin{pmatrix} \frac{474\,515\,843\,733}{12\,047\,257\,600\,000} \\ \frac{8\,371\,182\,426\,363}{12\,047\,257\,600\,000} \end{pmatrix} a^6 \right] \\
&- \frac{a}{5} \begin{pmatrix} \cos(2\theta) \\ \sin(2\theta) \end{pmatrix} \left[1 + \frac{1811}{5600} a^2 + \begin{pmatrix} \frac{24\,221\,269}{219\,520\,000} \\ \frac{62\,037\,019}{219\,520\,000} \end{pmatrix} a^4 + \begin{pmatrix} \frac{130\,045\,699\,263}{3\,442\,073\,600\,000} \\ \frac{868\,451\,160\,063}{3\,442\,073\,600\,000} \end{pmatrix} a^6 \right] \\
&- \frac{2\,a}{7} \begin{pmatrix} \cos(4\theta) \\ \sin(4\theta) \end{pmatrix} \left[1 + \frac{3851}{15\,680} a^2 + \frac{13\,443\,721}{115\,248\,000} a^4 + \begin{pmatrix} \frac{21\,617\,854\,235\,051}{289\,134\,182\,400\,000} \\ \frac{17\,348\,607\,323\,051}{289\,134\,182\,400\,000} \end{pmatrix} a^6 \right] \\
&+ \frac{55\,a^2}{448} \begin{pmatrix} \cos(5\theta) \\ \sin(5\theta) \end{pmatrix} \left[1 + \frac{8039}{16\,170} a^2 + \frac{12\,342\,441\,007}{40\,567\,296\,000} a^4 + \begin{pmatrix} \frac{170\,530\,641\,922\,939}{795\,119\,001\,600\,000} \\ \frac{157\,039\,154\,611\,189}{795\,119\,001\,600\,000} \end{pmatrix} a^6 \right] \\
&- \frac{11\,a^3}{192} \begin{pmatrix} \cos(6\theta) \\ \sin(6\theta) \end{pmatrix} \left(1 + \frac{64\,497}{86\,240} a^2 + \frac{7\,496\,313\,861}{13\,522\,432\,000} a^4 \right) \\
&+ \frac{847\,a^4}{30720} \begin{pmatrix} \cos(7\theta) \\ \sin(7\theta) \end{pmatrix} \left(1 + \frac{147\,961}{148\,225} a^2 + \frac{644\,679\,629\,761}{743\,733\,760\,000} a^4 \right) \\
&- \frac{517\,a^5}{38\,400} \begin{pmatrix} \cos(8\theta) \\ \sin(8\theta) \end{pmatrix} \left(1 + \frac{5\,060\,071}{4\,053\,280} a^2 \right) + \frac{10\,857\,a^6}{1\,638\,400} \begin{pmatrix} \cos(9\theta) \\ \sin(9\theta) \end{pmatrix} \left(1 + \frac{14\,804\,763}{9\,879\,870} a^2 \right) \\
&- \frac{13\,959\,a^7}{4\,259\,840} \begin{pmatrix} \cos(10\theta) \\ \sin(10\theta) \end{pmatrix} + \frac{15\,508\,449\,a^8}{9\,542\,041\,600} \begin{pmatrix} \cos(11\theta) \\ \sin(11\theta) \end{pmatrix} + O(a^9), \quad \text{(SM:3.3}e\text{)}
\end{aligned}$$

where the normalisation constants $N_{3;c/s}$, eigenvalues $\lambda_{3;c/s}$ and integrals $I_{c/s;0;3}$ are

given by:

$$\begin{aligned}
\begin{pmatrix} N_{3;c} \\ N_{3;s} \end{pmatrix} =& 1 + \frac{223\,a^2}{1225} + \frac{1\,199\,425\,259}{12\,293\,120\,000}a^4 + \begin{pmatrix} 32\,556\,442\,797\,593 \\ 38\,910\,282\,928\,343 \end{pmatrix} \frac{a^6}{542\,126\,592\,000\,000} \\
&+ \begin{pmatrix} 108\,883\,340\,088\,205\,146\,587 \\ 159\,714\,394\,135\,464\,282\,587 \end{pmatrix} \frac{a^8}{2\,720\,174\,388\,019\,200\,000\,000} + O(a^{10}), \\
\begin{pmatrix} \lambda_{3;c}^2 \\ \lambda_{3;s}^2 \end{pmatrix} =& 9 + \frac{9\,a^2}{70} + \frac{1\,093\,707}{10\,976\,000}a^4 + \begin{pmatrix} 10\,197\,202\,989 \\ 26\,873\,948\,739 \end{pmatrix} \frac{a^6}{215\,129\,600\,000} \\
&+ \begin{pmatrix} 220\,587\,681\,368\,967 \\ 1\,900\,963\,265\,932\,167 \end{pmatrix} \frac{a^8}{13\,492\,928\,512\,000\,000} + O(a^{10}), \\
I_{c;0;3} =& \frac{7\,a^3}{160\sqrt{2}} + \frac{19\,903\,a^5}{896\,000\sqrt{2}} + \frac{3\,315\,206\,799\,a^7}{280\,985\,600\,000\sqrt{2}} + O(a^9), \\
I_{s;0;3} =& -\frac{9\,a^2}{160\sqrt{2}} - \frac{23\,337\,a^4}{6\,272\,000\sqrt{2}} + \frac{3\,392\,103\,609\,a^6}{1\,966\,899\,200\,000\sqrt{2}} \\
&+ \frac{220\,940\,512\,414\,733\,a^8}{77\,102\,448\,640\,000\,000\sqrt{2}} + O(a^{10}),
\end{aligned} \tag{SM:3.3f}$$

The eigenfunctions corresponding to $n = 4$ are:

$$\begin{aligned}
&\frac{1}{\sqrt{2}(1 + a\cos\theta)} \begin{pmatrix} f_4/N_{4;c} \\ g_4/N_{4;s} \end{pmatrix} \\
&\quad = \begin{pmatrix} \cos(4\theta) \\ \sin(4\theta) \end{pmatrix} - \frac{a^3}{72} \begin{pmatrix} \cos(\theta) \\ \sin(\theta) \end{pmatrix} \left[1 + \begin{pmatrix} 2\,585 \\ 4\,937 \end{pmatrix} \frac{a^2}{4\,410} + \begin{pmatrix} \frac{60\,388\,801}{175\,032\,900} \\ \frac{190\,258\,009}{175\,032\,900} \end{pmatrix} a^4 \right] \\
&\quad + \frac{5\,a^2}{84} \begin{pmatrix} \cos(2\theta) \\ \sin(2\theta) \end{pmatrix} \left[1 + \frac{7\,747}{13\,230}a^2 + \begin{pmatrix} \frac{180\,740\,759}{525\,098\,700} \\ \frac{256\,977\,311}{525\,098\,700} \end{pmatrix} a^4 + \begin{pmatrix} \frac{46\,842\,519\,921\,871}{229\,252\,841\,433\,000} \\ \frac{103\,002\,862\,081\,639}{229\,252\,841\,433\,000} \end{pmatrix} a^6 \right] \\
&\quad - \frac{3\,a}{14} \begin{pmatrix} \cos(3\theta) \\ \sin(3\theta) \end{pmatrix} \left[1 + \frac{61}{196}a^2 + \frac{4\,266\,019}{23\,337\,720}a^4 + \begin{pmatrix} \frac{221\,583\,031\,597}{2\,037\,803\,034\,960} \\ \frac{309\,636\,249\,157}{2\,037\,803\,034\,960} \end{pmatrix} a^6 \right] \\
&\quad - \frac{5\,a}{18} \begin{pmatrix} \cos(5\theta) \\ \sin(5\theta) \end{pmatrix} \left(1 + \frac{2887}{11\,340}a^2 + \frac{124\,691\,197}{990\,186\,120}a^4 + \frac{1\,879\,098\,654\,779}{24\,562\,804\,439\,250}a^6 \right) \\
&\quad + \frac{7\,a^2}{60} \begin{pmatrix} \cos(6\theta) \\ \sin(6\theta) \end{pmatrix} \left(1 + \frac{44\,351}{87\,318}a^2 + \frac{1\,377\,470\,434}{4\,332\,064\,275}a^4 + \frac{3\,797\,335\,854\,506}{17\,193\,963\,107\,475}a^6 \right) \\
&\quad - \frac{637\,a^3}{11880} \begin{pmatrix} \cos(7\theta) \\ \sin(7\theta) \end{pmatrix} \left(1 + \frac{78\,367}{103\,194}a^2 + \frac{2\,928\,027\,962}{5\,119\,712\,325}a^4 \right) \\
&\quad + \frac{91\,a^4}{3564} \begin{pmatrix} \cos(8\theta) \\ \sin(8\theta) \end{pmatrix} \left(1 + \frac{260\,608}{257\,985}a^2 + \frac{94\,559\,197\,841}{106\,490\,016\,360}a^4 \right) \\
&\quad - \frac{49\,a^5}{3960} \begin{pmatrix} \cos(9\theta) \\ \sin(9\theta) \end{pmatrix} \left(1 + \frac{1\,300\,849}{1\,031\,940}a^2 \right) + \frac{259\,a^6}{42768} \begin{pmatrix} \cos(10\theta) \\ \sin(10\theta) \end{pmatrix} \left(1 + \frac{28\,843\,187}{19\,090\,890}a^2 \right) \\
&\quad - \frac{1\,739\,a^7}{583\,200} \begin{pmatrix} \cos(11\theta) \\ \sin(11\theta) \end{pmatrix} + \frac{50\,431\,a^8}{34\,214\,400} \begin{pmatrix} \cos(12\theta) \\ \sin(12\theta) \end{pmatrix} + O(a^9),
\end{aligned} \tag{SM:3.3g}$$

where the normalisation constants $N_{4;c/s}$, eigenvalues $\lambda_{4;c/s}$ and integrals $I_{c/s;0;4}$ are

given by:

$$\begin{aligned}
\begin{pmatrix} N_{4;c} \\ N_{4;s} \end{pmatrix} =& 1 + \frac{2929\,a^2}{15876} + \frac{1\,258\,094\,429\,a^4}{12\,602\,368\,800} + \frac{548\,970\,542\,700\,389\,a^6}{8\,069\,700\,018\,441\,600} \\
&+ \frac{a^8}{38\,434\,367\,247\,833\,652\,480\,000} \begin{pmatrix} 1\,914\,596\,975\,181\,836\,732\,371 \\ 2\,036\,610\,839\,460\,673\,724\,371 \end{pmatrix} + O(a^{10}), \\
\begin{pmatrix} \lambda^2_{4;c} \\ \lambda^2_{4;s} \end{pmatrix} =& 16 + \frac{8\,a^2}{63} + \frac{121\,202\,a^4}{1\,250\,235} + \frac{4\,494\,725\,731\,a^6}{54\,584\,009\,865} \\
&+ \frac{a^8}{21\,664\,393\,515\,418\,500} \begin{pmatrix} 1\,325\,696\,705\,088\,647 \\ 1\,860\,620\,001\,765\,647 \end{pmatrix} + O(a^{10}), \\
I_{c;0;4} =& -\frac{a^4}{72\sqrt{2}} - \frac{12\,235\,a^6}{1\,143\,072\sqrt{2}} - \frac{995\,564\,543\,a^8}{129\,624\,364\,800\sqrt{2}} + O(a^{10}), \\
I_{s;0;4} =& \frac{a^3}{63\sqrt{2}} + \frac{24\,041\,a^5}{5\,000\,940\sqrt{2}} + \frac{1\,111\,027\,697\,a^7}{793\,949\,234\,400\sqrt{2}} + O(a^9),
\end{aligned} \tag{SM:3.3h}$$

The diagonal elements $\mathsf{M}_{n,n}$, defined in Eq. (5.9) of the main text, are given by:

$$\begin{aligned}
\mathsf{M}_{1,1} =& \frac{a^2}{3} + \frac{25\,a^4}{108} + \frac{1\,933\,a^6}{10\,368} + \frac{358\,273\,a^8}{2\,239\,488} + O(a^{10}), \\
\mathsf{M}_{2,2} =& \frac{7\,a^2}{15} + \frac{1\,853\,a^4}{6\,750} + \frac{691\,021\,a^6}{3\,543\,750} + \frac{148\,782\,299\,a^8}{956\,812\,500} + O(a^{10}), \\
\mathsf{M}_{3,3} =& \frac{17\,a^2}{35} + \frac{60\,971\,a^4}{171\,500} + \frac{907\,888\,613\,a^6}{3\,361\,400\,000} + \frac{11\,165\,274\,765\,073\,a^8}{52\,706\,752\,000\,000} + O(a^{10}).
\end{aligned} \tag{SM:3.3i}$$

SM:3.1.2. *Eigenvalues for the viscosity term*

In this subsection we list the series solutions of Eq. (SM:3.1) for the case $\alpha = -3$. The even and odd eigenfunctions corresponding to $n = 1$ are:

$$\begin{aligned}
&\frac{(1 + a\cos\theta)^3}{\sqrt{2}} \begin{pmatrix} F_1/N_{1;c} \\ G_1/N_{1;s} \end{pmatrix} = \begin{pmatrix} \cos\theta \\ \sin\theta \end{pmatrix} \\
&\quad + a \begin{pmatrix} \cos(2\theta) \\ \sin(2\theta) \end{pmatrix} \left[1 + \begin{pmatrix} 31 \\ -1 \end{pmatrix} \frac{a^2}{32} + \begin{pmatrix} 4\,313 \\ -217 \end{pmatrix} \frac{a^4}{5120} + \begin{pmatrix} 478\,429 \\ -19\,459 \end{pmatrix} \frac{a^6}{819\,200} \right] \\
&\quad + \frac{9\,a^2}{32} \begin{pmatrix} \cos(3\theta) \\ \sin(3\theta) \end{pmatrix} \left[1 + \begin{pmatrix} 311 \\ 41 \end{pmatrix} \frac{a^2}{160} + \begin{pmatrix} 66\,883 \\ -893 \end{pmatrix} \frac{a^4}{25\,600} + \begin{pmatrix} 15\,933\,409 \\ -484\,545 \end{pmatrix} \frac{a^6}{5\,734\,400} \right] \\
&\quad + \frac{a^3}{80} \begin{pmatrix} \cos(4\theta) \\ \sin(4\theta) \end{pmatrix} \left[1 + \begin{pmatrix} 354 \\ 91 \end{pmatrix} \frac{a^2}{80} + \begin{pmatrix} 347\,213 \\ 15\,189 \end{pmatrix} \frac{a^4}{35\,840} \right] \\
&\quad - \frac{a^4}{1024} \begin{pmatrix} \cos(5\theta) \\ \sin(5\theta) \end{pmatrix} \left[1 + \begin{pmatrix} 1\,095 \\ 297 \end{pmatrix} \frac{a^2}{280} + \begin{pmatrix} 3\,417\,805 \\ 152\,013 \end{pmatrix} \frac{a^4}{501\,760} \right] \\
&+ \frac{27\,a^5}{179\,200} \begin{pmatrix} \cos(6\theta) \\ \sin(6\theta) \end{pmatrix} \left[1 + \begin{pmatrix} 5\,241 \\ 1\,577 \end{pmatrix} \frac{a^2}{1344} \right] - \frac{51\,a^6}{1\,638\,400} \begin{pmatrix} \cos(7\theta) \\ \sin(7\theta) \end{pmatrix} \left[1 + \begin{pmatrix} 91\,581 \\ 30\,595 \end{pmatrix} \frac{a^2}{22\,848} \right] \\
&\quad + \frac{153\,a^7}{20\,070\,400} \begin{pmatrix} \cos(8\theta) \\ \sin(8\theta) \end{pmatrix} - \frac{53\,703\,a^8}{25\,690\,112\,000} \begin{pmatrix} \cos(9\theta) \\ \sin(9\theta) \end{pmatrix} + O(a^9),
\end{aligned} \tag{SM:3.4a}$$

where the normalisation constants and the eigenvalues are given by:

$$\begin{aligned}
\begin{pmatrix} N_{1;c} \\ N_{1;s} \end{pmatrix} =& 1 + \begin{pmatrix} -5 \\ 1 \end{pmatrix} \frac{a^2}{4} + \begin{pmatrix} 3279 \\ 207 \end{pmatrix} \frac{a^4}{2048} - \begin{pmatrix} 1\,169\,319 \\ 3369 \end{pmatrix} \frac{a^6}{819\,200} \\
&+ \begin{pmatrix} 2\,404\,438\,743 \\ -35\,419\,433 \end{pmatrix} \frac{a^8}{1\,048\,576\,000} + O(a^{10}), \\
\begin{pmatrix} \chi^2_{1;c} \\ \chi^2_{1;s} \end{pmatrix} =& 1 + \begin{pmatrix} 9 \\ 3 \end{pmatrix} \frac{a^2}{4} + \begin{pmatrix} 207 \\ 15 \end{pmatrix} \frac{a^4}{128} + \begin{pmatrix} 19\,377 \\ -1\,233 \end{pmatrix} \frac{a^6}{20\,480} \\
&+ \begin{pmatrix} 694\,701 \\ -195\,411 \end{pmatrix} \frac{a^8}{3\,276\,800} + O(a^{10}), \\
\mathcal{I}_{c;1} =& -\frac{3\,a}{\sqrt{2}} - \frac{3\,a^3}{4\sqrt{2}} - \frac{5325\,a^5}{2048\sqrt{2}} + \frac{1\,143\,597\,a^7}{819\,200\sqrt{2}} + O(a^9), \\
\mathcal{I}_{s;1} =& \frac{1}{\sqrt{2}} + \frac{a^2}{4\sqrt{2}} - \frac{113\,a^4}{2048\sqrt{2}} - \frac{91\,529\,a^6}{819\,200\sqrt{2}} - \frac{57\,927\,593\,a^8}{1\,048\,576\,000\sqrt{2}} + O(a^{10}),
\end{aligned} \tag{SM:3.4b}$$

The eigenfunctions corresponding to $n = 2$ are:

$$\begin{aligned}
\frac{(1 + a\cos\theta)^3}{\sqrt{2}} \begin{pmatrix} F_2/N_{2;c} \\ G_2/N_{2;s} \end{pmatrix} =& \begin{pmatrix} \cos(2\theta) \\ \sin(2\theta) \end{pmatrix} \\
&+ \frac{a}{2} \begin{pmatrix} \cos(\theta) \\ \sin(\theta) \end{pmatrix} \left[1 - \frac{3}{5}a^2 - \begin{pmatrix} 33 \\ 8 \end{pmatrix} \frac{a^4}{125} - \begin{pmatrix} 4\,089 \\ 739 \end{pmatrix} \frac{a^6}{12\,500} \right] \\
&+ \frac{9\,a}{10} \begin{pmatrix} \cos(3\theta) \\ \sin(3\theta) \end{pmatrix} \left[1 + \frac{a^2}{25} + \frac{279}{1250}a^4 + \begin{pmatrix} 28\,303 \\ 9053 \end{pmatrix} \frac{a^6}{87\,500} \right] \\
&+ \frac{a^2}{5} \begin{pmatrix} \cos(4\theta) \\ \sin(4\theta) \end{pmatrix} \left[1 + \frac{11}{25}a^2 + \frac{2504}{4375}a^4 + \begin{pmatrix} 1\,199\,683 \\ 611\,683 \end{pmatrix} \frac{a^6}{1\,400\,000} \right] \\
&+ \frac{a^5}{140} \begin{pmatrix} \cos(5\theta) \\ \sin(5\theta) \end{pmatrix} \left(1 + \frac{1\,159}{800}a^2 \right) - \frac{9\,a^6}{11\,200} \begin{pmatrix} \cos(6\theta) \\ \sin(6\theta) \end{pmatrix} \left(1 + \frac{217}{150}a^2 \right) \\
&+ \frac{7\,a^7}{48\,000} \begin{pmatrix} \cos(7\theta) \\ \sin(7\theta) \end{pmatrix} - \frac{a^8}{30\,000} \begin{pmatrix} \cos(8\theta) \\ \sin(8\theta) \end{pmatrix} + O(a^9),
\end{aligned} \tag{SM:3.4c}$$

where the normalisation constants and the eigenvalues are given by:

$$\begin{aligned}
\begin{pmatrix} N_{2;c} \\ N_{2;s} \end{pmatrix} =& 1 + \frac{7a^2}{100} - \begin{pmatrix} 1\,798 \\ 1\,173 \end{pmatrix} \frac{a^4}{10\,000} - \begin{pmatrix} 362\,889 \\ 6\,014 \end{pmatrix} \frac{a^6}{1\,000\,000} \\
&- \begin{pmatrix} 740\,695\,061 \\ -91\,714\,314 \end{pmatrix} \frac{a^8}{1\,400\,000\,000} + O(a^{10}), \\
\begin{pmatrix} \chi^2_{2;c} \\ \chi^2_{2;s} \end{pmatrix} =& 4 + \frac{6\,a^2}{5} + \frac{126\,a^4}{125} + \begin{pmatrix} 7\,929 \\ 4\,179 \end{pmatrix} \frac{a^6}{6250} + \begin{pmatrix} 52\,917 \\ 10\,167 \end{pmatrix} \frac{a^8}{31\,250} + O(a^{10}) \\
\mathcal{I}_{c;2} =& \frac{3\,a^2}{2\sqrt{2}} + \frac{501\,a^4}{200\sqrt{2}} + \frac{69\,711\,a^6}{20\,000\sqrt{2}} + \frac{1\,095\,621\,a^8}{250\,000\sqrt{2}} + O(a^{10}), \\
\mathcal{I}_{s;2} =& -\frac{a}{\sqrt{2}} - \frac{77\,a^3}{100\sqrt{2}} - \frac{2111\,a^5}{5000\sqrt{2}} - \frac{118\,701\,a^7}{1\,000\,000\sqrt{2}} + O(a^9)
\end{aligned} \tag{SM:3.4d}$$

The eigenfunctions corresponding to $n = 3$ are:

$$
\begin{aligned}
\frac{(1+a\cos\theta)^3}{\sqrt{2}}\begin{pmatrix}F_3/N_{3;c}\\ G_3/N_{3;s}\end{pmatrix} &= \begin{pmatrix}\cos(3\theta)\\ \sin(3\theta)\end{pmatrix} \\
&+ \frac{3\,a^2}{160}\begin{pmatrix}\cos(\theta)\\ \sin(\theta)\end{pmatrix}\left[1-\begin{pmatrix}\frac{9\,691}{5\,600}\\ \frac{7\,941}{5\,600}\end{pmatrix}a^2-\begin{pmatrix}\frac{154\,340\,377}{439\,040\,000}\\ \frac{346\,420\,377}{439\,040\,000}\end{pmatrix}a^4-\begin{pmatrix}\frac{1\,194\,270\,293\,747}{5\,163\,110\,400\,000}\\ \frac{3\,050\,731\,639\,997}{5\,163\,110\,400\,000}\end{pmatrix}a^6\right] \\
&+ \frac{3\,a}{5}\begin{pmatrix}\cos(2\theta)\\ \sin(2\theta)\end{pmatrix}\left[1-\frac{343}{800}a^2-\begin{pmatrix}2\,276\,573\\ 2\,950\,323\end{pmatrix}\frac{a^4}{31\,360\,000}-\begin{pmatrix}\frac{159\,364\,862\,017}{1\,475\,174\,400\,000}\\ \frac{799\,005\,790\,085}{7\,375\,872\,000\,000}\end{pmatrix}a^6\right] \\
&+ \frac{6\,a}{7}\begin{pmatrix}\cos(4\theta)\\ \sin(4\theta)\end{pmatrix}\left[1-\frac{817}{15\,680}a^2+\frac{16\,100\,807}{115\,248\,000}a^4+\begin{pmatrix}\frac{27\,121\,790\,334\,503}{289\,134\,182\,400\,000}\\ \frac{244\,516\,963\,701\,521}{2\,023\,939\,276\,800\,000}\end{pmatrix}a^6\right] \\
&+ \frac{75\,a^2}{448}\begin{pmatrix}\cos(5\theta)\\ \sin(5\theta)\end{pmatrix}\left[1+\frac{2041}{7350}a^2+\frac{6\,782\,829\,737}{18\,439\,680\,000}a^4+\begin{pmatrix}\frac{1\,319\,142\,046\,324\,451}{3\,975\,595\,008\,000\,000}\\ \frac{1\,537\,502\,350\,890\,701}{3\,975\,595\,008\,000\,000}\end{pmatrix}a^6\right] \\
&- \frac{5\,a^3}{1344}\begin{pmatrix}\cos(6\theta)\\ \sin(6\theta)\end{pmatrix}\left[1-\frac{27\,813}{39\,200}a^2-\frac{63\,903\,588\,831}{67\,612\,160\,000}a^4\right] \\
&+ \frac{a^4}{2048}\begin{pmatrix}\cos(7\theta)\\ \sin(7\theta)\end{pmatrix}\left(1-\frac{1721}{2695}a^2-\frac{70\,050\,165\,701}{67\,612\,160\,000}a^4\right) \\
&- \frac{19\,a^5}{197\,120}\begin{pmatrix}\cos(8\theta)\\ \sin(8\theta)\end{pmatrix}\left(1-\frac{361\,007}{744\,800}a^2\right)+\frac{589\,a^6}{25\,231\,360}\begin{pmatrix}\cos(9\theta)\\ \sin(9\theta)\end{pmatrix}\left(1-\frac{5\,594\,091}{18\,759\,650}a^2\right) \\
&- \frac{2945\,a^7}{459\,210\,752}\begin{pmatrix}\cos(10\theta)\\ \sin(10\theta)\end{pmatrix}+\frac{35\,929\,a^8}{18\,702\,401\,536}\begin{pmatrix}\cos(11\theta)\\ \sin(11\theta)\end{pmatrix}+O(a^9), \quad \text{(SM:3.4}e\text{)}
\end{aligned}
$$

where the normalisation constants and the eigenvalues are given by:

$$
\begin{aligned}
\begin{pmatrix}N_{3;c}\\ N_{3;s}\end{pmatrix} =& 1+\frac{339\,a^2}{2450}-\frac{670\,144\,221}{12\,293\,120\,000}a^4-\begin{pmatrix}30\,708\,394\,950\,253\\ 41\,642\,251\,826\,503\end{pmatrix}\frac{a^6}{542\,126\,592\,000\,000} \\
&- \begin{pmatrix}22\,705\,450\,573\,027\,956\,877\\ 21\,719\,992\,990\,220\,916\,877\end{pmatrix}\frac{a^8}{302\,241\,598\,668\,800\,000\,000}+O(a^{10}), \\
\begin{pmatrix}\chi^2_{3;c}\\ \chi^2_{3;s}\end{pmatrix} =& 9+\frac{81\,a^2}{70}+\frac{10\,004\,067\,a^4}{10\,976\,000}+\begin{pmatrix}161\,791\,474\,881\\ 184\,670\,003\,631\end{pmatrix}\frac{a^6}{215\,129\,600\,000} \\
&+ \begin{pmatrix}9\,504\,660\,124\,760\,247\\ 10\,794\,030\,777\,176\,247\end{pmatrix}\frac{a^8}{13\,492\,928\,512\,000\,000}+O(a^{10}), \\
\mathcal{I}_{c;3} =& -\frac{121\,a^3}{160\sqrt{2}}-\frac{8\,624\,187\,a^5}{6\,272\,000\sqrt{2}}-\frac{3\,773\,553\,410\,799\,a^7}{1\,966\,899\,200\,000\sqrt{2}}+O(a^7), \\
\mathcal{I}_{s;3} =& \frac{99\,a^2}{160\sqrt{2}}+\frac{4\,478\,823\,a^4}{6\,272\,000\sqrt{2}}+\frac{1\,363\,121\,741\,781\,a^6}{1\,966\,899\,200\,000\sqrt{2}} \\
&+ \frac{47\,148\,574\,938\,227\,333\,a^8}{77\,102\,448\,640\,000\,000\sqrt{2}}+O(a^{10}), \quad \text{(SM:3.4}f\text{)}
\end{aligned}
$$

The eigenfunctions corresponding to $n = 4$ are:

$$\begin{aligned}
\frac{(1+a\cos\theta)^3}{\sqrt{2}}\begin{pmatrix}F_4/N_{4;c}\\ G_4/N_{4;s}\end{pmatrix} &= \begin{pmatrix}\cos(4\theta)\\ \sin(4\theta)\end{pmatrix} \\
&\quad - \frac{a^3}{280}\begin{pmatrix}\cos(\theta)\\ \sin(\theta)\end{pmatrix}\left[1 - \begin{pmatrix}1\,129\\ 541\end{pmatrix}\frac{a^2}{1\,470} - \begin{pmatrix}2\,592\,461\\ 3\,108\,431\end{pmatrix}\frac{a^4}{6\,482\,700}\right] \\
&\quad + \frac{a^2}{28}\begin{pmatrix}\cos(2\theta)\\ \sin(2\theta)\end{pmatrix}\left[1 - \frac{1297}{1470}a^2 - \begin{pmatrix}2\,453\,441\\ 2\,064\,479\end{pmatrix}\frac{a^4}{6\,482\,700} - \begin{pmatrix}90\,110\,373\,169\\ 96\,485\,460\,349\end{pmatrix}\frac{a^6}{314\,475\,777\,000}\right] \\
&\quad + \frac{9\,a}{14}\begin{pmatrix}\cos(3\theta)\\ \sin(3\theta)\end{pmatrix}\left[1 - \frac{215}{588}a^2 - \frac{134\,431}{2\,593\,080}a^4 - \begin{pmatrix}\frac{9\,526\,796\,561}{125\,790\,310\,800}\\ \frac{144\,696\,279\,826}{1\,761\,064\,351\,200}\end{pmatrix}a^6\right] \\
&\quad + \frac{5\,a}{6}\begin{pmatrix}\cos(5\theta)\\ \sin(5\theta)\end{pmatrix}\left(1 - \frac{17}{180}a^2 + \frac{187\,513}{1\,746\,360}a^4 + \frac{5\,523\,205\,229}{77\,014\,476\,000}a^6\right) \\
&\quad + \frac{3\,a^2}{20}\begin{pmatrix}\cos(6\theta)\\ \sin(6\theta)\end{pmatrix}\left(1 + \frac{269}{1386}a^2 + \frac{17\,239\,469}{61\,122\,600}a^4 + \frac{179\,351\,057\,909}{700\,831\,731\,600}a^6\right) \\
&\quad - \frac{7\,a^3}{1320}\begin{pmatrix}\cos(7\theta)\\ \sin(7\theta)\end{pmatrix}\left(1 - \frac{13}{63}a^2 - \frac{19\,194\,293}{72\,235\,800}a^4\right) \\
&\quad + \frac{a^4}{1320}\begin{pmatrix}\cos(8\theta)\\ \sin(8\theta)\end{pmatrix}\left(1 - \frac{59}{585}a^2 - \frac{3\,031\,739}{10\,319\,400}a^4\right) \\
&\quad - \frac{9\,a^5}{57200}\begin{pmatrix}\cos(9\theta)\\ \sin(9\theta)\end{pmatrix}\left(1 + \frac{17}{252}a^2\right) + \frac{19\,a^6}{480\,480}\begin{pmatrix}\cos(10\theta)\\ \sin(10\theta)\end{pmatrix}\left(1 + \frac{21\,971}{83\,790}a^2\right) \\
&\quad - \frac{57\,a^7}{5\,096\,000}\begin{pmatrix}\cos(11\theta)\\ \sin(11\theta)\end{pmatrix} + \frac{1539\,a^8}{448\,448\,000}\begin{pmatrix}\cos(12\theta)\\ \sin(12\theta)\end{pmatrix} + O(a^9), \quad \text{(SM:3.4}g\text{)}
\end{aligned}$$

where the normalisation constants and the eigenvalues are given by:

$$\begin{aligned}
\begin{pmatrix}N_{4;c}\\ N_{4;s}\end{pmatrix} &= 1 + \frac{283a^2}{1764} - \frac{4\,011\,409\,a^4}{155\,584\,800} - \frac{385\,712\,253\,103\,a^6}{11\,069\,547\,350\,400} \\
&\quad - \begin{pmatrix}202\,339\,939\,883\,471\,309\\ 244\,789\,123\,790\,003\,789\end{pmatrix}\frac{a^8}{5\,858\,004\,457\,831\,680\,000} + O(a^{10}), \\
\begin{pmatrix}\chi^2_{4;c}\\ \chi^2_{4;s}\end{pmatrix} &= 16 + \frac{8\,a^2}{7} + \frac{13\,598\,a^4}{15\,435} + \frac{56\,779\,561\,a^6}{74\,875\,185} \\
&\quad + \begin{pmatrix}2\,197\,706\,056\,367\\ 2\,343\,263\,416\,007\end{pmatrix}\frac{a^8}{3\,301\,995\,658\,500} + O(a^{10}), \\
\mathcal{I}_{c;4} &= \frac{27\,a^4}{70\sqrt{2}} + \frac{53\,433\,a^6}{68\,600\sqrt{2}} + \frac{463\,131\,007\,a^8}{403\,368\,000\sqrt{2}} + O(a^{10}), \\
\mathcal{I}_{s;4} &= -\frac{12\,a^3}{35\sqrt{2}} - \frac{12\,589\,a^5}{25\,725\sqrt{2}} - \frac{250\,425\,647\,a^7}{453\,789\,000\sqrt{2}} + O(a^9). \qquad \text{(SM:3.4}h\text{)}
\end{aligned}$$

SM:3.2. *Eigenfunctions for $a = 1$*

This section discusses the analytical solutions of Eq. (SM:3.1) for the limiting case of $a = 1$.

SM:3.2.1. *Eigenfunctions for the inviscid case*

When $a = 1$, the integration weight $(1 + a\cos\theta)^{-1}$ in Eq. (3.11) of the main text diverges as $\theta \to \pi$. The even solutions must therefore be proportional to a power of $1+\cos\theta$. For this reason, the zeroth order even mode $f_0 = (1-a^2)^{1/4}$, corresponding to $\lambda^2_{c;n} = 0$, must be excluded from the set of mode solutions.

Introducing $f_n = (1 + a\cos\theta)^\alpha \widetilde{f}_n$, we rewrite Eq. (3.15) with respect to the variable $u = (1+\cos\theta)/2$:

$$u(1-u)\frac{d^2\widetilde{f}_n}{du^2} + \left(2\alpha - \frac{1}{2} - 2\alpha u\right)\frac{d\widetilde{f}_n}{du} + \left[\lambda^2_{c;n} - \alpha(\alpha-1) + \frac{\alpha}{u}\left(\alpha - \frac{3}{2}\right)\right]\widetilde{f}_n = 0. \tag{SM:3.8}$$

In order for the solution to be regular around $u = 0$, it is necessary for the coefficient of u^{-1} to vanish. This selects the value $\alpha = 3/2$ and the above equation becomes that of the hypergeometric function (Olver *et al.* 2010):

$$u(1-u)\frac{d^2\widetilde{f}}{du^2} + [c - (a+b+1)u]\frac{d\widetilde{f}}{du} - ab\widetilde{f} = 0, \tag{SM:3.9}$$

where $c = \frac{5}{2}$, $a = 1 + \sqrt{\lambda^2_{c;n} + \frac{1}{4}}$ and $b = 1 - \sqrt{\lambda^2_{c;n} + \frac{1}{4}}$. Since c is not an integer, the general solution is the linear combination

$$\widetilde{f} = A\,{}_2F_1(a, b; c; u) + Bu^{1-c}\,{}_2F_1(a-c+1, b-c+1; 2-c; u). \tag{SM:3.10}$$

Since $1 - c = -\frac{3}{2}$, the prefactor in the second term cancels the $(1+\cos\theta)^\alpha$ factor which allows f to have finite norm. Thus, this term must be discarded by setting $B = 0$. Turning the attention now towards the first term, we note that close to $u = 1$, we have

$${}_2F_1\left(1+\nu, 1-\nu; \frac{5}{2}; 1-\delta u\right) = \frac{3\cos\nu\pi}{1-4\nu^2} - \frac{3\sin\nu\pi}{2\nu}\sqrt{\delta u} + O(\delta u), \tag{SM:3.11}$$

where $\sqrt{\delta u} = |\sin(\theta/2)|$. While the above expression allows the limit $\theta \to 0$ of f_n to be obtained, the derivative of f_n is in general not well defined, since

$$\lim_{\theta\to 0\pm} \partial_\theta \sqrt{\frac{1-\cos\theta}{2}} = \lim_{\theta\to 0\pm} \frac{\sin\theta}{4|\sin(\theta/2)|}, \tag{SM:3.12}$$

which is $\pm 1/2$ depending on the direction from which 0 is approached. The only way to obtain a differentiable solution is to cancel the coefficient of $\sqrt{\delta u}$, by setting $\nu = \sqrt{\lambda^2 + 1/4}$ to an integer value $n = 1, 2, \ldots$. This gives the following eigenfrequency spectrum:

$$\lambda^2_{c;n} = n^2 - \frac{1}{4}, \tag{SM:3.13}$$

while the normalised eigenfunctions are

$$\begin{aligned}\lim_{a\to 1} f_n(\theta) =& (1+\cos\theta)^{3/2}\frac{(-1)^{n+1}n}{3}\sqrt{2(4n^2-1)}\,{}_2F_1\left(1+n, 1-n; \frac{5}{2}; \frac{1+\cos\theta}{2}\right)\\ =& (1+\cos\theta)^{3/2}\sqrt{2(4n^2-1)}\sum_{j=0}^{n-1}\frac{(-1)^{n-j-1}(n+j)!}{j!(n-j-1)!(2j+3)!!}(1+\cos\theta)^j.\end{aligned} \tag{SM:3.14}$$

The first few functions in the set are listed below:

$$\begin{aligned} f_1(\theta) =& \sqrt{\frac{2}{3}}(1+\cos\theta)^{3/2}, \\ f_2(\theta) =& 2\sqrt{\frac{2}{15}}(1+\cos\theta)^{3/2}(3\cos\theta-2), \\ f_3(\theta) =& \sqrt{\frac{2}{35}}(1+\cos\theta)^{3/2}(20\cos^2\theta-16\cos\theta-1), \\ f_4(\theta) =& \frac{4}{3}\sqrt{\frac{2}{7}}(1+\cos\theta)^{3/2}(14\cos^3\theta-12\cos^2\theta-3\cos\theta+2). \end{aligned} \tag{SM:3.15}$$

The odd solutions of Eq. (3.10) in the limit $a \to 1$ have much simpler expressions:

$$g_n(\theta) = \sqrt{\frac{n+1}{n}}\sin(n\theta) + \sqrt{\frac{n}{n+1}}\sin[(n+1)\theta]. \tag{SM:3.16}$$

The discrete eigenvalues corresponding to the odd modes g_n are

$$\lambda_{s;n} = \sqrt{n(n+1)}. \tag{SM:3.17}$$

The results in Eqs. (SM:3.13) and (SM:3.17) are shown in Fig. 2 of the main text as horizontal lines, indicating the $a \to 1$ limits of $\lambda_{c;n}$ and $\lambda_{s;n}$ for $n = 1$, 2 and 3.

SM:3.2.2. *Eigenfunctions for the viscosity term*

As in the previous subsection, Eq. (4.5) of the main text can be rewritten in the hypergeometric form, by switching to the variable $u = (1+\cos\theta)/2$:

$$\begin{aligned} u(1-u)\frac{d^2F_n}{du^2} + \left(\frac{7}{2}-4u\right)\frac{dF_n}{du} + \chi^2_{c;n}F_n =& 0, \\ u(1-u)\frac{d^2\widetilde{G}_n}{du^2} + \left(\frac{7}{2}-5u\right)\frac{d\widetilde{G}_n}{du} + \left(\chi^2_{s;n}-\frac{7}{4}\right)\widetilde{G}_n =& 0, \end{aligned} \tag{SM:3.18}$$

where $\widetilde{G}$ is defined through

$$G(\theta) = \frac{\sin\theta}{\sqrt{1+\cos\theta}}\widetilde{G}(\theta). \tag{SM:3.19}$$

Comparing Eq. (SM:3.18) with Eq. (SM:3.9), we find $a = \frac{3}{2} - \sqrt{\chi^2+\frac{9}{4}}$, $b = \frac{3}{2} + \sqrt{\chi^2+\frac{9}{4}}$ and $c = 7/2$ for F_n and $a = 2 - \sqrt{\chi^2+\frac{9}{4}}$, $b = 2 + \sqrt{\chi^2+\frac{9}{4}}$ and $c = 7/2$ for G_n. Since $1-c = -5/2$ in both cases, the second solution in Eq. (SM:3.10) diverges when $\theta = \pi$ and $u = 0$. The continuity of the solution and its derivative is guaranteed when $a = -n$ is a non-positive integer ($n = 0, 1, \dots$), such that the allowed eigenvalues are

$$\chi^2_{c;n} = n(n+3), \qquad \chi^2_{s;n} = \left(n+\frac{5}{2}\right)\left(n-\frac{1}{2}\right). \tag{SM:3.20}$$

These limiting values for the eigenvalues are shown with horizontal lines in Fig. 8 of the main text.

When $n = 0$, the odd mode is not defined, while the even mode is given by Eq. (4.7), i.e. $F_0(\theta) = \sqrt{2/5}$. Imposing unit norm with respect to the inner product in Eq. (4.6),

we find

$$
\begin{aligned}
F_n(\theta) =& \frac{(-1)^n(2n+3)}{15}\sqrt{(n+1)(n+2)(2n+1)(2n+5)}{}_2F_1\left(-n, 3+n; \frac{7}{2}; \frac{1+\cos\theta}{2}\right) \\
=& (2n+3)\sqrt{\frac{(2n+1)(2n+5)}{(n+1)(n+2)}}\sum_{j=0}^{n}\frac{(-1)^{n-j}(n+j+2)!(1+\cos\theta)^j}{j!(n-j)!(2j+5)!!}, \\
\widetilde{G}_n(\theta) =& \frac{(-1)^{n+1}(n+1)}{15}\sqrt{2n(n+2)(2n+1)(2n+3)}{}_2F_1\left(1-n, 3+n; \frac{7}{2}; \frac{1+\cos\theta}{2}\right) \\
=& \sqrt{\frac{2(2n+1)(2n+3)}{n(n+2)}}\sum_{j=0}^{n-1}\frac{(-1)^{n+1-j}(n+j+2)!(1+\cos\theta)^j}{j!(n-j-1)!(2j+5)!!},
\end{aligned}
\tag{SM:3.21}
$$

The first few eigenfunctions $F_n(\theta)$ and $G_n(\theta)$ are

$$
\begin{aligned}
F_1(\theta) =& \sqrt{\frac{2}{7}}(4\cos\theta - 3), \qquad G_1(\theta) = \sqrt{\frac{8}{5}}\frac{\sin\theta}{\sqrt{1+\cos\theta}}, \\
F_2(\theta) =& \frac{2}{\sqrt{15}}(10\cos^2\theta - 10\cos\theta + 1), \qquad G_2(\theta) = \frac{4}{\sqrt{35}}\frac{\sin\theta}{\sqrt{1+\cos\theta}}(5\cos\theta - 2), \\
F_3(\theta) =& \frac{2}{\sqrt{385}}(112\cos^3\theta - 126\cos^2\theta + 6\cos\theta + 13), \\
G_3(\theta) =& \frac{8}{\sqrt{210}}\frac{\sin\theta}{\sqrt{1+\cos\theta}}\left(14\cos^2\theta - 8\cos\theta - 1\right).
\end{aligned}
\tag{SM:3.22}
$$

REFERENCES

Ambruș, V. E., Busuioc, S., Wagner, A. J., Paillusson, F. & Kusumaatmaja, H. 2019 Multicomponent flow on curved surfaces: A vielbein lattice Boltzmann approach. *Phys. Rev. E* **100**, 063306.

Jiang, G. S. & Shu, C. W. 1996 Efficient implementation of weighted eno schemes. *J. Comput. Phys.* **126**, 202.

Olver, F. W. J., Lozier, D. W., Boisvert, R. F. & Clark, C. W. 2010 *NIST handbook of mathematical functions*. New York, NY: Cambridge University Press.

Radice, D. & Rezzolla, L. 2012 THC: A new high high-order finite-difference high-resolution shock-capturing code for special-relativistic hydrodynamics. *Astron. Astrophys.* **547**, A26.

Rezzolla, L. & Zanotti, O. 2013 *Relativistic hydrodynamics*. Oxford University Press.

Shu, C. W. 1997 Essentially non-oscillatory and weighted essentially non-oscillatory schemes for hyperbolic conservation laws. In *Advances numerical approximation of nonlinear hyperbolic equations* (ed. A. Quarteroni), *Lecture notes in mathematics*, vol. 1697, pp. 325–432. Springer.

Shu, C.-W. & Osher, S. 1988 Efficient implementation of essentially non-oscillatory shock-capturing schemes. *J. Comput. Phys.* **77**, 439–471.

Toro, E. F. 2009 *Riemann solvers and numerical methods for fluid dynamics*, 3rd edn. Springer.

Zhang, W. & MacFadyen, A. I. 2006 RAM: A relativistic adaptive mesh refinement hydrodynamics code. *Astrophys. J. Suppl. S.* **164**, 255–279.